HCl gel electrophoresis (BIO-RAD, CA, USA) and blotted to polyvinylidene difluoride membranes (Millipore, MA, USA). The following primary antibodies were used in this study; anti-pERK1/2 (1:500), anti-pAkt (1:500), anti-ERK2 (1:500) and anti-Akt (1:500). All experiments were repeated at least three times with similar results. Representative data are shown. Results are expressed as percentage of control values by normalization of relative density of pERK1/2/total ERK2, and pAkt/total Akt to those from untreated conditions of each experiment.

2.9. Statistical analysis

Clinical and demyelination scores were analyzed by nonparametric methods Kruskal–Wallis or Mann–Whitney tests, as specified in the text or figure legends. Results from grip strength measurement, quantitative histologic analysis, and electrophysiology are expressed as mean ± SEM. Unless otherwise specified, statistical significance was determined by analysis of variance (ANOVA) followed by Student's *t* test and the Bonferroni method for multiple group experiments.

3. Results

3.1. Effect of FTY720 on disease severity in SAP

To examine possible therapeutic effects of FTY720 in SAP, animals were treated with FTY720 (0.3 mg/kg) ($n=5$), FTY720 (1 mg/kg) ($n=10$) or water (control, $n=11$) orally once daily at 7 mo of age (anticipated disease onset) for 4 weeks. At 7 mo (before treatment), there was no difference in median clinical scores amongst 3 groups. As shown in Fig. 1A, animals treated with water or FTY720 (0.3 mg/kg) exhibited worsening of clinical scores at 8 mo. By comparison, disease progression was significantly inhibited in animals treated with FTY720 (1 mg/kg), which was also reflected in grip strength measurements (Fig. 1B). Subsequent analysis was focused only in the FTY720 (1 mg/kg) group.

Electrophysiology and histologic studies were performed in a subset of study animals at 8 mo. Our previous studies in SAP mice (7–8 mo old) revealed that sciatic motor responses had prolonged distal latencies, slowed conduction velocities, and decreased amplitudes compared to those recorded from age-matched wild type NOD mice (Salomon et al., 2001). These observations were confirmed in this study. Distal latency was 3.1 ± 0.5 ms; conduction velocity was 15.5 ± 3.3 m/s; and amplitude was 1.46 ± 0.36 mV in untreated 7 mo old SAP mice ($n=8$). Values obtained from the water-treated group at 8 mo were similar to those recorded from untreated mice. As shown in Fig. 1C and D, there was a significant improvement in the distal latency and conduction velocity but not in the amplitude of the motor response in the FTY720 (1 mg/kg) group ($n=7$) compared to water-treated group ($n=6$).

Histological analysis by a blinded observer revealed a milder loss of myelinated fibers and lesser degree of demyelination in epon sections from FTY720-treated mice compared to those from water-treated group (Fig. 2A). The total number of myelinated axons/mm^2 was 10,533 ± 1992 in sections from water-treated mice, and 14,996 ± 1663 in sections from FTY720-treated group. Compared to unaffected nerves from preclinical mice, there was a 40.8 ± 12.8% ($n=6$) decrease in myelinated fibers in water-treated mice, and 10 ± 4.7% ($n=7$) decrease in FTY720-treated group ($p< 0.015$ by *t* test). In addition to the loss of myelinated axons, there were more demyelinated or thinly myelinated fibers in water-treated ones compared to FTY720-treated group. The median demyelination score was 2 for water vs 0.5 for FTY720 ($p<0.0.014$ by Mann–Whitney test). H & E staining revealed that there was a decrease in the extent of inflammatory infiltrates in nerve sections from FTY720-treated

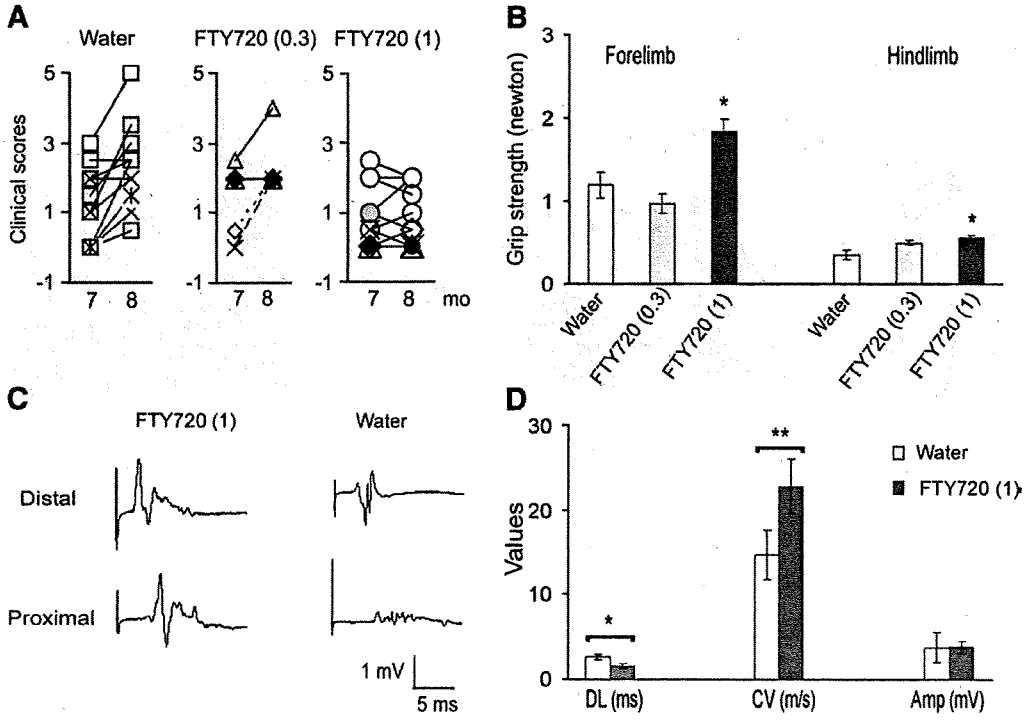

Fig. 1. Suppression of SAP in B7-2 deficient NOD mice by FTY720. Animals were divided into 3 groups: (1) water ($n=11$); (2) FTY720 at 0.3 mg/kg ($n=5$); and (3) FTY720 at 1.0 mg/kg ($n=10$). Daily oral administration was initiated at 7 months of age and continued for 4 weeks. A. Clinical scores. The median clinical score at 8 mo was 2.5 for water-treated group, 2.0 for FTY720 (0.3 mg/kg) and 0.75 for FTY720 (1 mg/kg); *p< 0.0006 for FTY720 (1 mg/kg) vs water (Mann–Whitney test). B. Hindlimb and forelimb grip strength measurements. *p< 0.01 for FTY720 (1 mg/kg) vs water. C, D. Examples and summary of sciatic nerve electrophysiology. Distal latency (DL), conduction velocity (CV), and amplitude (Amp) of sciatic compound muscle action potentials (CMAPs) were measured [$n=7$ mice for FTY720 (1 mg/kg) group, and $n=6$ for water-treated ones; *p< 0.02; **p< 0.01]. Subsequent analysis was carried out in FTY720 (1 mg/kg) group only.

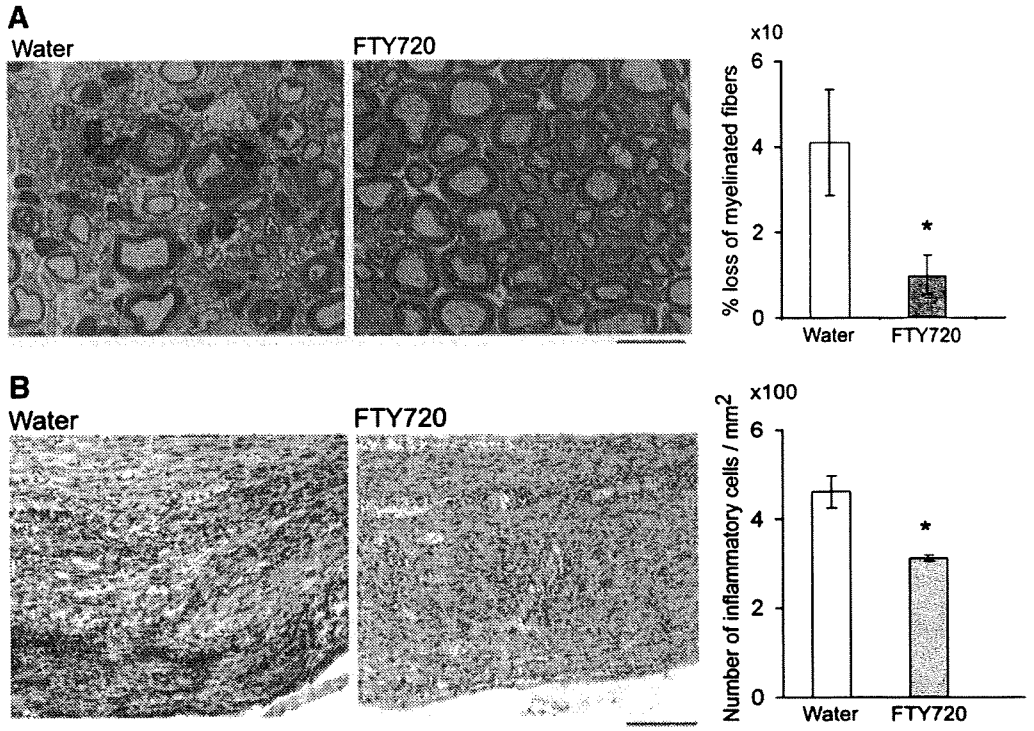

Fig. 2. FTY720 attenuates the severity of sciatic nerve pathology in SAP mice. A. Examples of epon sections from sciatic nerves of SAP mice treated with water or FTY720. Loss of myelinated fibers was attenuated in FTY720-treated mice compared to water-treated mice ($*p < 0.015$). Scale bar represents 20 μm. B. Examples of H &E sections of sciatic nerves showing decreased inflammatory cell infiltrates in FTY720-treated animals compared to water-treated ones ($*p < 0.02$). Scale bar represents 100 μm. For A and B, $n = 7$ for FTY720 group and $n = 6$ for the water group.

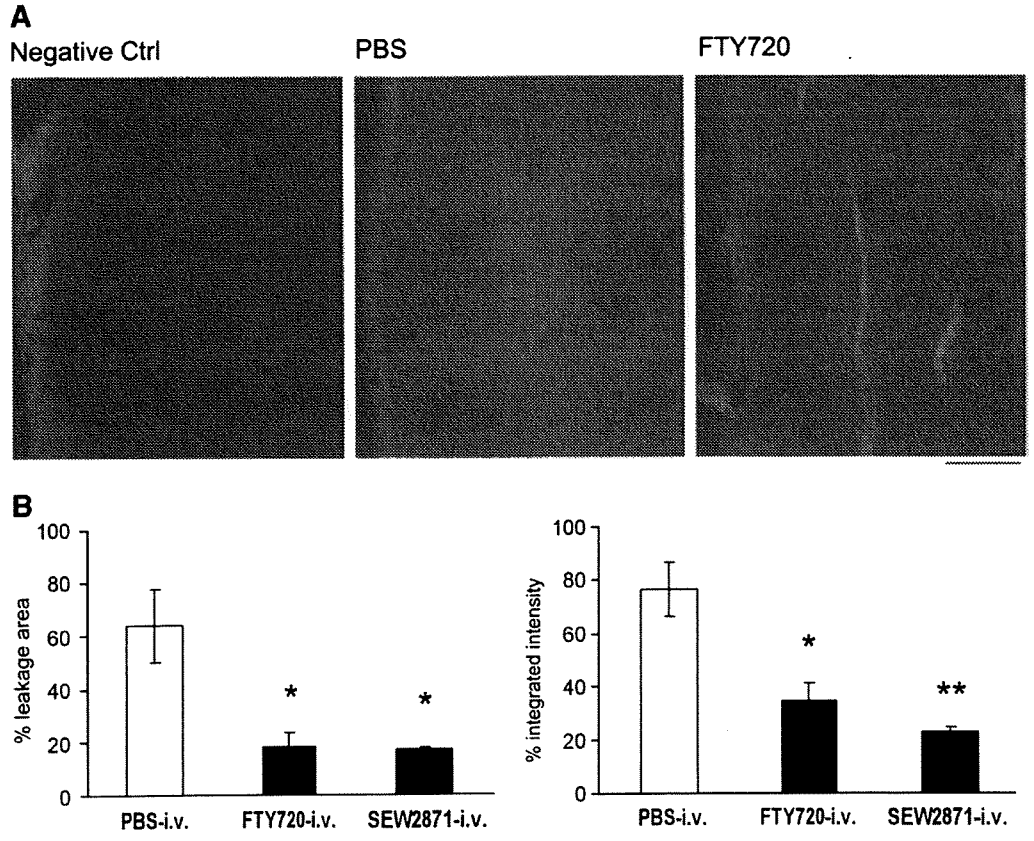

Fig. 3. Inhibition of blood nerve barrier (BNB) permeability by FTY720 in SAP mice. A. Examples of nerve sections from mice given Evans blue albumin (i.v.) 6 h after a single dose of intravenous FTY720, SEW2871 or PBS. Animals were sacrificed 30 min after Evans blue. Scale bar represents 100 μm. B. Data summary ($n = 3$ each). * For % leakage area, $p < 0.02$ for PBS vs FTY720 or SEW2871; for % integrated intensity, $*p < 0.02$ for PBS vs FTY720, $**p < 0.005$ for PBS vs SEW2871.

group compared to sections from water-treated ones, as shown in Fig. 2B. Thus, clinical, electrophysiological and histologic findings indicate that FTY720 treatment ameliorates the severity of SAP.

3.2. Mechanisms of action of FTY720 and SEW2871 in SAP

3.2.1. Effect on the blood nerve barrier (BNB)

Both functional S1P1 agonism on endothelial cells and functional antagonism at lymphocyte S1P1 receptors play a role in the attenuation of lymphocyte infiltration into target organs (Brinkmann, 2007). We investigated whether a single injection of FTY720 could prevent or attenuate the disruption of the BNB and whether a selective S1P1 agonist SEW2871 could mimic the effect. Sciatic nerve sections of PBS-treated mice showed leakage of EBA from microvessels into the surrounding endoneurium and perineurium; whereas the fluorescence of EBA remained within endoneurial microvessels in nerve sections from FTY720 and SEW2871-treated mice (Fig. 3A, B). These data indicate that S1P receptor modulators rapidly inhibit the disruption of the BNB via S1P1 on endothelial cells.

Given the above findings, we examined whether SEW2871 could also ameliorate the clinical severity of SAP. B7-2 KO NOD mice at 7 mo of age were administered SEW2871 or 4% DMSO (control) by oral gavage for 4 weeks. At 8 mo, clinical scores worsened in the DMSO group ($n=7$), but not in SEW2871-treated mice ($n=8$) (Fig. 4A). There was no decline in grip strength in SEW2871-treated animals, in contrast to that observed in DMSO-treated mice (Fig. 4B). Furthermore, sciatic nerve conduction studies revealed a significant difference in distal latency, conduction velocity and amplitude of the motor response in SEW2871-treated mice compared with control mice (Fig. 4C).

3.2.2. Effect on autoreactivity to myelin P0

We have recently reported that myelin P0 is one of the autoantigens in SAP, which is Th1-mediated (Kim et al., 2008). We examined the proliferative and cytokine responses of splenocytes isolated from control, FTY720- or SEW2871-gavaged mice. Treatment with FTY720 or SEW2871 led to a decrease in the proliferative response of splenocytes to P0 (180–199) compared to those from control mice. There was no response to OVA (323–339) and P2 (53–78) in all mice (Fig. 5A). IL-2 and IFN-γ levels were also decreased in splenocyte supernatants from FTY720- or SEW2871-gavaged mice compared to control mice (Fig. 5B). No significant effect on IL-10 or IL-17 levels was noted ($n=3$–4, not shown). In contrast, exposure of cultured splenocytes for 48 h to FTY720P (10–100 nM) or SEW2871 (100 nM) did not alter Th1 cytokine responses to P0 (180–199) ($n=3$, not shown). Mice treated with FTY720 or SEW2871 had increased percentage of $CD4^+Foxp3^+$ T cells and $CD4^+CD25^+Foxp3^+$ T cells in spleens and lymph nodes (LNs) compared to vehicle-treated mice (Fig. 5C). These results suggest that S1P receptor modulators tilt the balance in favor of regulatory T cells (Tregs) than effector T cells in B7-2 KO NOD mice.

3.2.3. Potential trophic/protective effect on Schwann cells

Real-time PCR studies revealed that S1P receptors are expressed by neonatal rat SCs with a relative mRNA level of S1P3>S1P2-S1P1>S1P4=S1P5 (Fig. 6A). Given the above, we investigated whether the active form of FTY720 (FTY720P) would exert gliioprotective action or promote glial regeneration that could be pertinent in SAP. Treatment of SCs for 3 days with FTY720P in differentiating medium (0.5% FBS + ITS + forskolin) had no effect on SC differentiation based on P0 protein levels ($n=3$, data not shown). When serum withdrawal was used to induce cell death, the percentage of trypan $blue^+$ cells was decreased by FTY720P treatment (Fig. 6B). Western blot analysis showed that exposure of rat SCs to FTY720P (15 min) stimulated the phosphorylation of ERK1/2 (2.8 fold, $n=5$) and Akt (1.6 fold, $n=6$) compared to controls (Fig. 6C). However, we could not

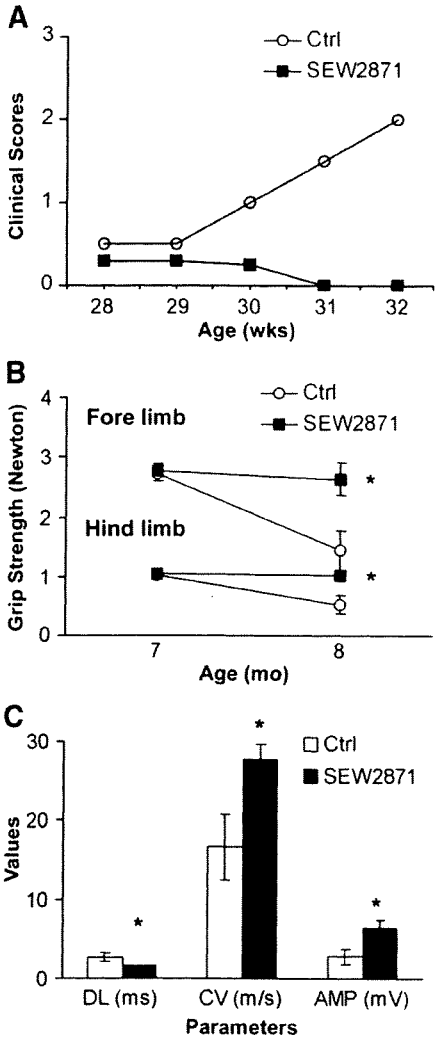

Fig. 4. Amelioration of SAP by SEW2871. SEW2871 (10 mg/kg) was given orally twice a day at 7 months of age and continued for 4 weeks. A. Median clinical scores ($n=7$ for Ctrl; $n=8$ for SEW2871). B. Grip strength measurements. * $p<0.007$ for SEW2871 vs Ctrl in forelimb at 8 mo, and $p<0.008$ in hindlimb. C. Data summary of electrophysiology at 8 mo ($n=6$ for Ctrl; $n=8$ for SEW2871). * $p<0.02$ for DL and CV; $p<0.03$ in Amp. In B and C, one vehicle-treated mouse died before grip strength measurements and electrophysiologic studies could be performed.

detect a difference in apoptotic ($TUNEL^+$) cells in nerve sections from FTY720-treated mice compared to those from control mice, possibly due to low frequency of $TUNEL^+$ cells at this particular time point (8 mo) (not shown).

4. Discussion

FTY720, a prototype of S1P receptor modulators, acts acutely as an agonist at S1P receptors when phosphorylated to yield FTY720P, but preferentially desensitizes the $S1P_1$ receptor subtype upon prolonged exposure (functional antagonism). Not all lymphocyte subsets are affected equally. FTY720 induces a preferential depletion of naïve and central memory T cells but not effector memory T cells from the peripheral circulation of MS patients (Mehling et al., 2008). FTY720 also regulates B cell and dendritic cell migration (Cinamon et al., 2008; Lan et al., 2005). S1P1 activation induces an anti-inflammatory phenotype in macrophages and prevents monocyte-endothelial interactions (Hughes et al., 2008; Whetzel et al., 2006). These findings, taken together, suggest that therapeutic actions of FTY720

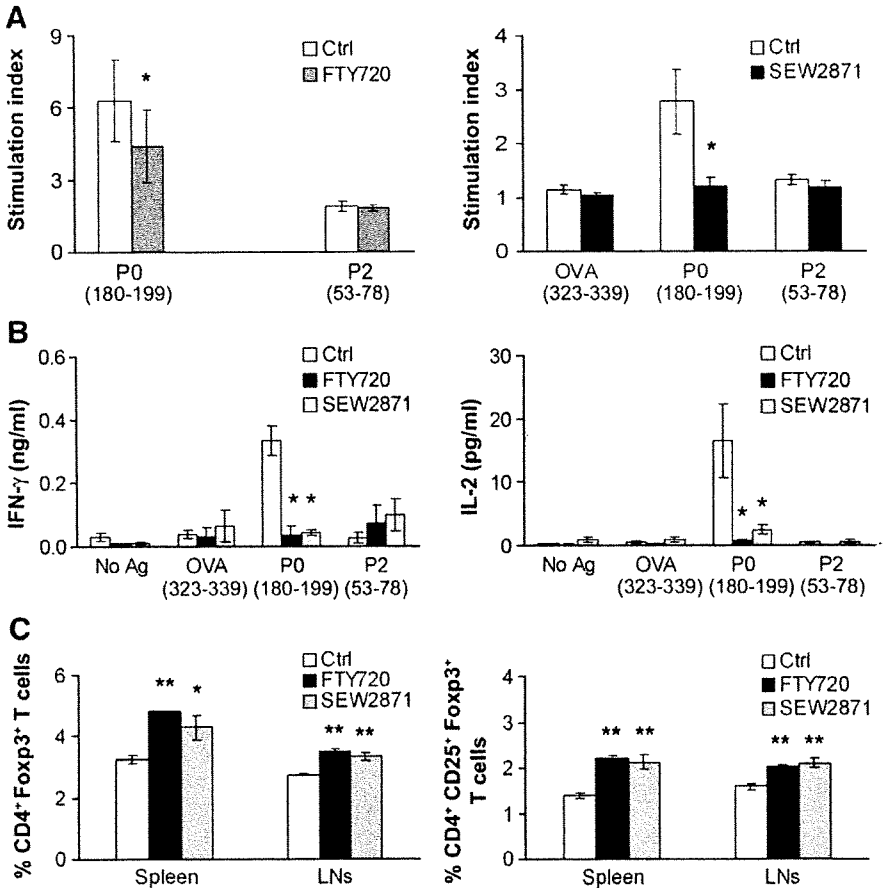

Fig. 5. Effect of FTY720 or SEW2871 treatment on P0 autoreactivity and on Tregs in SAP. A. The proliferative response to P0 (180–199) was decreased in splenocytes from FTY720- or SEW2871-treated mice ($n = 3$–4 each). *$p < 0.01$ for FTY720 vs Ctrl; $p < 0.02$ for SEW2871 vs Ctrl. B. Cytokine responses of splenocytes to the same Ags in replicate culture ($n = 7$ for Ctrl; $n = 3$ for FTY720; $n = 4$ for SEW2871). IFN-γ and IL-2 secretion were decreased in splenocytes from FTY720- or SEW2871 gavaged mice. *$p < 0.003$ for FTY720 or SEW2871 vs Ctrl for IFN-γ; $p < 0.05$ for FTY720 vs Ctrl or SEW2871 vs Ctrl for IL-2. C. There was an increase in the percentage of Tregs in spleens and LNs of FTY720- or SEW2871-gavaged mice compared to Ctrl ($n = 3$–5 each). *$p < 0.01$ for SEW2871vs Ctrl in spleen; ** the rest: $p < 0.001$ for FTY720 or SEW2871 vs Ctrl.

and related compounds could be extended to inflammatory diseases affecting the peripheral nervous system.

Preclinical studies are usually carried out in two or more animal models of the disease to demonstrate consistent response across species or models. Regarding autoimmune neuropathies, EAN can be induced by myelin proteins such as P0, P2 or by galactocerebroside in rodents and rabbits respectively, as reviewed previously (Hahn, 1996). More recently, we and other investigators found that spontaneous autoimmune neuropathy in B7-2 KO NOD mice is mediated by P0, although possible contributions from other antigens in disease progression cannot be excluded (Kim et al., 2008; Louvet et al., 2009). To our knowledge, there have been no studies of FTY720 or SEW2871 in a spontaneous model of inflammatory neuropathy or multiple sclerosis. We found that FTY720 treatment given at disease onset halted the progression of SAP in B7-2 KO NOD mice, which was confirmed by histological and electrophysiological findings. The rapid inhibition of the BNB by FTY720 and SEW2871 in SAP demonstrates the crucial role of S1P1 receptors on endothelial cells in autoimmune diseases. A two photon imaging study of living T cells also revealed that S1P1 agonist prevents lymphocytes from crossing into medullary sinuses, though it does not distinguish between actions at endothelial S1P1 vs lymphocyte S1P1 (Wei et al., 2005). SEW2871, like FTY720, halted the progression of SAP, though it is less potent as an agonist, has a shorter duration of action, and differs in S1P receptor fate after internalization. FTY720P and AFD-R induce S1P1 receptor degradation, while SEW2871 and the physiologic ligand S1P induce receptor recycling, which correlates with the extent of ubiquitination (Gonzalez-Cabrera et al., 2007; Oo et al., 2007).

It is thought that effector mechanisms may not be affected by S1P receptor modulators (Brinkmann et al., 2002). The effector phase of SAP is mediated by Th1 cytokines, although there is an increase in IL-17 transcripts during the preclinical phase (Bour-Jordan et al., 2005; Kim et al., 2008). We found that FTY720P or SEW2871 had no direct effects on Th1 cytokine responses in vitro, yet splenocytes from FTY720-treated and SEW2871-treated SAP mice exhibited a decreased proliferative and/or Th1 cytokine response to myelin P0. Our observations may simply reflect FTY720-induced T cell depletion from the spleen and the circulation (Hofmann et al., 2006). Another possibility consists of indirect inhibition of pathogenic T cell expansion by S1P receptor modulators via increased number or function of Tregs. Indeed, we found increased number of Tregs in spleens and LNs of FTY720- or SEW2871-gavaged mice. Other investigators have reported that Tregs exhibit a reduced chemotaxis to S1P compared to other T cells, and that Tregs from FTY720-treated mice, but not those from vehicle-treated mice, could inhibit airway inflammation in C57BL/6 mice (Sawicka et al., 2005).

Aside from immune cells, neurons and glial cells also express S1P receptors, albeit differing in the predominating receptor subtypes. We found that Schwann cells express S1P3 > S1P2 > S1P1 > S1P4 = S1P5, in contrast to cells of oligodendroglial lineage where S1P1 and S1P5 predominate (Jaillard et al., 2005; Jung et al., 2007). Other investigators reported that S1P1 is expressed by terminal SCs but

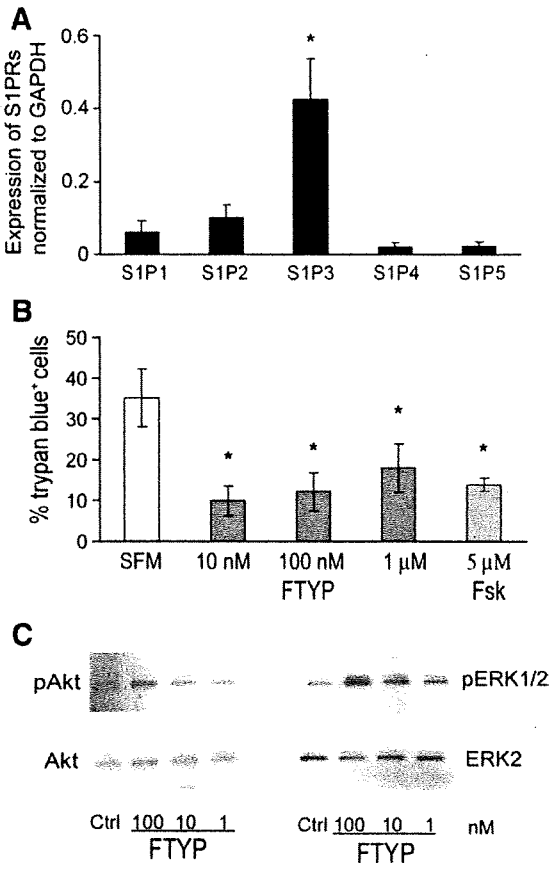

Fig. 6. Direct effects of FTY720P on cultured Schwann cells. A. S1P receptor mRNA levels relative to expression of GAPDH mRNA ($R = 2^{-\Delta CT}$) in SCs. *$p < 0.005$ for S1P3 vs other S1P receptors in rat SCs ($n = 3$). B. FTY720P rescues SCs from serum withdrawal-induced cell death. SCs were treated with 1 nM, 10 nM, 100 nM FTY720P (FTYP) or 5 μM forskolin (Fsk) ($n = 4$–5 each). *$p < 0.02$ for each treatment compared with serum-free medium (SFM). C. Representative examples of Western blot analysis demonstrating that exposure to FTY720P for 15 min stimulates the phosphorylation of ERK1/2 and Akt in rat SCs.

not by myelinating SCs, whereas S1P2, S1P3 and S1P4 receptors are expressed by both SC subtypes (Kobashi et al., 2006). S1P activates Rac1 and RhoA and increases SC migration (Barber et al., 2004). We found that FTY720P improves SC survival in vitro as well as activates both ERK2 and Akt pathways, which regulate SC survival, proliferation and differentiation (Hila et al., 2001; Ogata et al., 2004). FTY720P does not enhance SC differentiation as determined by P0 expression. Whether S1P receptor modulators modulate the function of SCs or axons in vivo is unclear and would require investigations in non-autoimmune neuropathies.

In summary, we found that both FTY720 and SEW2871 exert therapeutic actions in SAP, with acute effects mediated by functional agonism at S1P1 receptors of endothelial cells, followed by complex effects on the immune system characterized by T cell depletion with relative sparing of Tregs. Our data indicate that modulation of S1P1 receptors is sufficient to induce a protective effect on autoimmunity, but do not exclude possible contributions from other S1P receptors. One recognizes the limitations of SAP and EAN as animal models of autoimmune neuropathies given that previous attempts found only low frequency of humoral or cellular responses to myelin P0, P2 or glycolipids in human CIDP, perhaps reflecting epitope spreading or the heterogeneity of the disease. Nonetheless, our results suggest a potential therapeutic role for S1P receptor modulators in CIDP and other inflammatory neuropathies based on their actions on BNB permeability and differential sequestration of lymphocyte subsets.

Acknowledgements

We thank Shawna Cook for her assistance in the project. This work was supported by the National Institute of Health Grant R21 NS049014, Miller Group Charitable Trust Fund (Mr. M.P. Miller III), and Jack Miller Center for Peripheral Neuropathy. B7-2 KO NOD mice were generously provided by Dr. Jeffrey A. Bluestone (University of California, San Francisco). FTY720 was generously provided by Novartis (Basel, Switzerland). Potential conflict of interest: nothing to report.

References

Allende, M.L., Sasaki, T., Kawai, H., Olivera, A., Mi, Y., van Echten-Deckert, G., Hajdu, R., Rosenbach, M., Keohane, C.A., Mandala, S., Spiegel, S., Proia, R.L., 2004. Mice deficient in sphingosine kinase 1 are rendered lymphopenic by FTY720. J. Biol. Chem. 279, 52487–52492.

Balatoni, B., Storch, M.K., Swoboda, E.M., Schonborn, V., Koziel, A., Lambrou, G.N., Hiestand, P.C., Weissert, R., Foster, C.A., 2007. FTY720 sustains and restores neuronal function in the DA rat model of MOG-induced experimental autoimmune encephalomyelitis. Brain Res. Bull. 74, 307–316.

Barber, S.C., Mellor, H., Gampel, A., Scolding, N.J., 2004. S1P and LPA trigger Schwann cell actin changes and migration. Eur. J. Neurosci. 19, 3142–3150.

Bour-Jordan, H., Thompson, H.L., Bluestone, J.A., 2005. Distinct effector mechanisms in the development of autoimmune neuropathy versus diabetes in nonobese diabetic mice. J. Immunol. 175, 5649–5655.

Brinkmann, V., 2007. Sphingosine 1-phosphate receptors in health and disease: mechanistic insights from gene deletion studies and reverse pharmacology. Pharmacol. Ther. 115, 84–105.

Brinkmann, V., Davis, M.D., Heise, C.E., Albert, R., Cottens, S., Hof, R., Bruns, C., Prieschl, E., Baumruker, T., Hiestand, P., Foster, C.A., Zollinger, M., Lynch, K.R., 2002. The immune modulator FTY720 targets sphingosine 1-phosphate receptors. J. Biol. Chem. 277, 21453–21457.

Chiba, K., Yanagawa, Y., Masubuchi, Y., Kataoka, H., Kawaguchi, T., Ohtsuki, M., Hoshino, Y., 1998. FTY720, a novel immunosuppressant, induces sequestration of circulating mature lymphocytes by acceleration of lymphocyte homing in rats. I. FTY720 selectively decreases the number of circulating mature lymphocytes by acceleration of lymphocyte homing. J. Immunol. 160, 5037–5044.

Cinamon, G., Zachariah, M.A., Lam, O.M., Foss Jr., F.W., Cyster, J.G., 2008. Follicular shuttling of marginal zone B cells facilitates antigen transport. Nat. Immunol. 9, 54–62.

Coelho, R.P., Payne, S.G., Bittman, R., Spiegel, S., Sato-Bigbee, C., 2007. The immunomodulator FTY720 has a direct cytoprotective effect in oligodendrocyte progenitors. J. Pharmacol. Exp. Ther. 323, 626–635.

Foster, C.A., Mechtcheriakova, D., Storch, M.K., Balatoni, B., Howard, L.M., Bornancin, F., Wlachos, A., Sobanov, J., Kinnunen, A., Baumruker, T., 2009. FTY720 rescue therapy in the dark agouti rat model of experimental autoimmune encephalomyelitis: expression of central nervous system genes and reversal of blood-brain-barrier damage. Brain Pathol. 29, 254–266.

Fujino, M., Funeshima, N., Kitazawa, Y., Kimura, H., Amemiya, H., Suzuki, S., Li, X.K., 2003. Amelioration of experimental autoimmune encephalomyelitis in Lewis rats by FTY720 treatment. J. Pharmacol. Exp. Ther. 305, 70–77.

Gonzalez-Cabrera, P.J., Hla, T., Rosen, H., 2007. Mapping pathways downstream of sphingosine 1-phosphate subtype 1 by differential chemical perturbation and proteomics. J. Biol. Chem. 282, 7254–7264.

Graler, M.H., Goetzl, E.J., 2004. The immunosuppressant FTY720 down-regulates sphingosine 1-phosphate G-protein-coupled receptors. Faseb J. 18, 551–553.

Hadden, R.D., Sharrack, B., Bensa, S., Soudain, S.E., Hughes, R.A., 1999. Randomized trial of interferon beta-1a in chronic inflammatory demyelinating polyradiculoneuropathy. Neurology 53, 57–61.

Hahn, A.F., 1996. Experimental allergic neuritis (EAN) as a model for the immune-mediated demyelinating neuropathies. Rev. Neurol. (Paris) 152, 328–332.

Hila, S., Soane, L., Koski, C.L., 2001. Sublytic C5b-9-stimulated Schwann cell survival through PI 3-kinase-mediated phosphorylation of BAD. Glia 36, 58–67.

Hofmann, M., Brinkmann, V., Zerwes, H.G., 2006. FTY720 preferentially depletes naive T cells from peripheral and lymphoid organs. Int. Immunopharmacol. 6, 1902–1910.

Hughes, J.E., Srinivasan, S., Lynch, K.R., Proia, R.L., Ferdek, P., Hedrick, C.C., 2008. Sphingosine-1-phosphate induces an antiinflammatory phenotype in macrophages. Circ. Res. 102, 950–958.

Iwase, T., Jung, C.G., Bae, H., Zhang, M., Soliven, B., 2005. Glial cell line-derived neurotrophic factor-induced signaling in Schwann cells. J. Neurochem. 94, 1488–1499.

Jaillard, C., Harrison, S., Stankoff, B., Aigrot, M.S., Calver, A.R., Duddy, G., Walsh, F.S., Pangalos, M.N., Arimura, N., Kaibuchi, K., Zalc, B., Lubetzki, C., 2005. Edg8/S1P5: an oligodendroglial receptor with dual function on process retraction and cell survival. J. Neurosci. 25, 1459–1469.

Jung, C.G., Kim, H.J., Miron, V.E., Cook, S., Kennedy, T.E., Foster, C.A., Antel, J.P., Soliven, B., 2007. Functional consequences of S1P receptor modulation in rat oligodendroglial lineage cells. Glia 55, 1656–1667.

Kappos, L., Antel, J., Comi, G., Montalban, X., O'Connor, P., Polman, C.H., Haas, T., Korn, A. A., Karlsson, G., Radue, E.W., 2006. Oral fingolimod (FTY720) for relapsing multiple sclerosis. N. Engl. J. Med. 355, 1124–1140.

Kim, H.J., Jung, C.G., Jensen, M.A., Dukala, D., Soliven, B., 2008. Targeting of myelin protein zero in a spontaneous autoimmune polyneuropathy. J. Immunol. 181, 8753–8760.

Kobashi, H., Yaoi, T., Oda, R., Okajima, S., Fujiwara, H., Kubo, T., Fushiki, S., 2006. Lysophospholipid receptors are differentially expressed in rat terminal Schwann cells, as revealed by a single cell rt-PCR and in situ hybridization. Acta Histochem. Cytochem. 39, 55–60.

Lan, Y.Y., De Creus, A., Colvin, B.L., Abe, M., Brinkmann, V., Coates, P.T., Thomson, A.W., 2005. The sphingosine-1-phosphate receptor agonist FTY720 modulates dendritic cell trafficking in vivo. Am. J. Transplant 5, 2649–2659.

Louvet, C., Kabre, B.G., Davini, D.W., Martinier, N., Su, M.A., DeVoss, J.J., Rosenthal, W.L., Anderson, M.S., Bour-Jordan, H., Bluestone, J.A., 2009. A novel myelin P0-specific T cell receptor transgenic mouse develops a fulminant autoimmune peripheral neuropathy. J. Exp. Med. 206, 507–514.

Maeda, Y., Matsuyuki, H., Shimano, K., Kataoka, H., Sugahara, K., Chiba, K., 2007. Migration of CD4 T cells and dendritic cells toward sphingosine 1-phosphate (S1P) is mediated by different receptor subtypes: S1P regulates the functions of murine mature dendritic cells via S1P receptor type 3. J. Immunol. 178, 3437–3446.

Mandala, S., Hajdu, R., Bergstrom, J., Quackenbush, E., Xie, J., Milligan, J., Thornton, R., Shei, G.J., Card, D., Keohane, C., Rosenbach, M., Hale, J., Lynch, C.L., Rupprecht, K., Parsons, W., Rosen, H., 2002. Alteration of lymphocyte trafficking by sphingosine-1-phosphate receptor agonists. Science 296, 346–349.

Matloubian, M., Lo, C.G., Cinamon, G., Lesneski, M.J., Xu, Y., Brinkmann, V., Allende, M.L., Proia, R.L., Cyster, J.G., 2004. Lymphocyte egress from thymus and peripheral lymphoid organs is dependent on S1P receptor 1. Nature 427, 355–360.

Mehling, M., Brinkmann, V., Antel, J., Bar-Or, A., Goebels, N., Vedrine, C., Kristofic, C., Kuhle, J., Lindberg, R.L., Kappos, L., 2008. FTY720 therapy exerts differential effects on T cell subsets in multiple sclerosis. Neurology 71, 1261–1267.

Miron, V.E., Hall, J.A., Kennedy, T.E., Soliven, B., Antel, J.P., 2008. Cyclical and dose-dependent responses of adult human mature oligodendrocytes to fingolimod. Am. J. Pathol. 173, 1143–1152.

Nagano, S., Takeda, M., Ma, L., Soliven, B., 2001. Cytokine-induced cell death in immortalized Schwann cells: roles of nitric oxide and cyclic AMP. J. Neurochem. 77, 1486–1495.

Ogata, T., Iijima, S., Hoshikawa, S., Miura, T., Yamamoto, S., Oda, H., Nakamura, K., Tanaka, S., 2004. Opposing extracellular signal-regulated kinase and Akt pathways control Schwann cell myelination. J. Neurosci. 24, 6724–6732.

Oo, M.L., Thangada, S., Wu, M.T., Liu, C.H., Macdonald, T.L., Lynch, K.R., Lin, C.Y., Hla, T., 2007. Immunosuppressive and anti-angiogenic sphingosine 1-phosphate receptor-1 agonists induce ubiquitinylation and proteasomal degradation of the receptor. J. Biol. Chem. 282, 9082–9089.

Pinschewer, D.D., Ochsenbein, A.F., Odermatt, B., Brinkmann, V., Hengartner, H., Zinkernagel, R.M., 2000. FTY720 immunosuppression impairs effector T cell peripheral homing without affecting induction, expansion, and memory. J. Immunol. 164, 5761–5770.

Salomon, B., Rhee, L., Bour-Jordan, H., Hsin, H., Montag, A., Soliven, B., Arcella, J., Girvin, A.M., Padilla, J., Miller, S.D., Bluestone, J.A., 2001. Development of spontaneous autoimmune peripheral polyneuropathy in B7-2-deficient NOD mice. J. Exp. Med. 194, 677–684.

Sawicka, E., Dubois, G., Jarai, G., Edwards, M., Thomas, M., Nicholls, A., Albert, R., Newson, C., Brinkmann, V., Walker, C., 2005. The sphingosine 1-phosphate receptor agonist FTY720 differentially affects the sequestration of CD4+/CD25+ T-regulatory cells and enhances their functional activity. J. Immunol. 175, 7973–7980.

Setoguchi, R., Hori, S., Takahashi, T., Sakaguchi, S., 2005. Homeostatic maintenance of natural Foxp3(+) CD25(+) CD4(+) regulatory T cells by interleukin (IL)-2 and induction of autoimmune disease by IL-2 neutralization. J. Exp. Med. 201, 723–735.

Vallat, J.M., Hahn, A.F., Leger, J.M., Cros, D.P., Magy, L., Tabaraud, F., Bouche, P., Preux, P. M., 2003. Interferon beta-1a as an investigational treatment for CIDP. Neurology 60, S23–28.

Webb, M., Tham, C.S., Lin, F.F., Lariosa-Willingham, K., Yu, N., Hale, J., Mandala, S., Chun, J., Rao, T.S., 2004. Sphingosine 1-phosphate receptor agonists attenuate relapsing-remitting experimental autoimmune encephalitis in SJL mice. J. Neuroimmunol. 153, 108–121.

Wei, S.H., Rosen, H., Matheu, M.P., Sanna, M.G., Wang, S.K., Jo, E., Wong, C.H., Parker, I., Cahalan, M.D., 2005. Sphingosine 1-phosphate type 1 receptor agonism inhibits transendothelial migration of medullary T cells to lymphatic sinuses. Nat. Immunol. 6, 1228–1235.

Whetzel, A.M., Bolick, D.T., Srinivasan, S., Macdonald, T.L., Morris, M.A., Ley, K., Hedrick, C.C., 2006. Sphingosine-1 phosphate prevents monocyte/endothelial interactions in type 1 diabetic NOD mice through activation of the S1P1 receptor. Circ. Res. 99, 731–739.

Zhang, Z., Zhang, Z.Y., Fauser, U., Schluesener, H.J., 2008. FTY720 ameliorates experimental autoimmune neuritis by inhibition of lymphocyte and monocyte infiltration into peripheral nerves. Exp. Neurol. 210, 681–690.

Journal of Neurochemistry

JNC

JOURNAL OF NEUROCHEMISTRY | 2009 | 110 | 791–800

doi: 10.1111/j.1471-4159.2009.06175.x

Proinflammatory cytokine interferon-γ increases induction of indoleamine 2,3-dioxygenase in monocytic cells primed with amyloid β peptide 1–42: implications for the pathogenesis of Alzheimer's disease

Akiko Yamada,* Hidetoshi Akimoto,* Syota Kagawa,* Gilles J. Guillemin† and Osamu Takikawa*

*National Institute for Longevity Sciences, National Center for Geriatrics and Gerontology, Aichi, Japan

†Centre for Immunology, St. Vincent's Hospital, Sydney, Australia

Abstract

Indoleamine 2,3-dioxygenase (IDO) is the rate-limiting enzyme of the kynurenine pathway of tryptophan metabolism, ultimately leading to production of the excitotoxin quinolinic acid (QUIN) by monocytic cells. In the Tg2576 mouse model of Alzheimer's disease, systemic inflammation induced by lipopolysaccharide leads to an increase in IDO expression and QUIN production in microglia surrounding amyloid plaques. We examined whether the IDO over-expression in microglia could be mediated by brain proinflammatory cytokines induced during the peripheral inflammation using THP-1 cells and peripheral blood mononuclear cells (PBMC) as models for microglia. THP-1 cells pre-treated with 5–25 μM amyloid β peptide (Aβ) (1–42) but not with Aβ (1–40) or Aβ (25–35) became an activated state as indicated by their morphological changes and enhanced adhesiveness. IDO expression was only slightly increased in the reactive cells but strongly enhanced following treatment with proinflammatory cytokine interferon-γ (IFN-γ) but not with interleukin-1β, tumor necrosis factor-α, or interleukin-6 at 100 U/mL. The concomitant addition of Aβ (1–42) with IFN-γ was totally ineffective, indicating that Aβ pre-treatment is prerequisite for a high IDO expression. The priming effect of Aβ (1–42) for the IDO induction was also observed for PBMC. These findings suggest that IFN-γ induces IDO over-expression in the primed microglia surrounding amyloid plaques.

Keywords: Alzheimer's disease, amyloid β peptide, indoleamine 2,3 dioxygenase, microglia, proinflammatory cytokine, quinolinic acid.

J. Neurochem. (2009) **110**, 791–800.

The kynurenine pathway (KP) is the major route of tryptophan metabolism, leading to the production of NAD or the complete oxidation for energy production (Fig. 1). Indoleamine 2,3-dioxygease (IDO) and tryptophan 2,3-dioxygenase represent the first and rate-limiting enzyme in the KP (Takikawa *et al.* 1986; Takikawa 2005). IDO is known to be induced during various neuroinflammatory diseases and this induction causes the marked elevation of several neurotoxic metabolites including the free radical generator 3-hydroxykynurenine and the excitotoxic NMDA receptor agonist quinolinic acid (QUIN) in the brain (Heyes *et al.* 1992; Moroni 1999; Stone *et al.* 2001; Smith *et al.* 2007). The brain IDO induction also elevates the concentrations of NMDA receptor antagonist, kynurenine (Kyn), but generally to a lesser extent than the increases in QUIN (Heyes *et al.* 1992; Naritsin *et al.* 1995). Therefore, dysregulation of the KP, mainly associated with an over-expression of IDO, has been implicated in the pathogenesis of neuroinflammatory and neurodegenerative disorders, such as Huntington's disease (Pearson and Reynolds 1992; Stoy *et al.* 2005), Parkinson's disease (Ogawa *et al.* 1992), amyotrophic lateral sclerosis (Guillemin *et al.* 2005a), and AIDS dementia complex (Heyes *et al.* 1992).

Received November 9, 2008; revised manuscript received April 27, 2009; accepted April 27, 2009.

Address correspondence and reprint requests to Osamu Takikawa, National Institute for Longevity Sciences, National Center for Geriatrics and Gerontology, 36-3 Gengo, Morioka, Obu, Aichi 474-8522, Japan. E-mail: takikawa@nils.go.jp

Abbreviations used: AD, Alzheimer's disease; Aβ, amyloid β peptide; GM-CSF, granulocyte macrophage-colony stimulating factor; IDO, indoleamine 2,3-dioxygenase; IFN, interferon; IL-18, interleukin-18; KP, kynurenine pathway; Kyn, kynurenine; mAb, monoclonal antibody; PBMC, pheripheral blood mononuclear cells; PBS, phosphate-buffered saline; qRT-PCR, quantitative RT-PCR; QUIN, quinolinic acid; TDO, tryptophan 2,3-dioxygenase; TNF-α, tumor necrosis factor-α.

© 2009 The Authors
Journal Compilation © 2009 International Society for Neurochemistry,

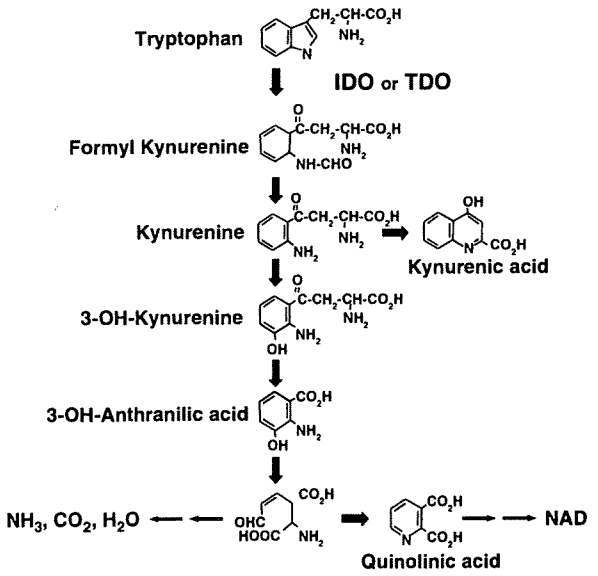

Fig. 1 The kynurenine pathway (KP) of tryptophan metabolism. IDO and tryptophan 2,3-dioxygenase (TDO) represent the first and rate-limiting enzymes in the KP.

Alzheimer's disease (AD) is the leading cause of dementia (Selkoe 2001). The pathological hallmarks of AD are extracellular amyloid plaques, intracellular neurofibrillary tangles, and dystrophic neurites (Selkoe 2001; Morgan *et al.* 2004). Amyloid β (Aβ) peptides consisting of 40 or 42 amino acid residues represent a primary component of amyloid plaques. Aβ (1–42) is considered to be the most neurotoxic form of the peptides (Drouet *et al.* 2000). Aβ (1–42) can activate primary cultured human microglia and induce IDO expression (Guillemin *et al.* 2003; Walker *et al.* 2006). Furthermore, IDO over-expression and increased production of QUIN have been observed in microglia associated with amyloid plaques in the brains of AD patients (Guillemin *et al.* 2005b). Thus, over-expression of IDO and over-activation of the KP in microglia are likely to be involved in the pathogenesis of AD.

We have previously studied the potential role of the KP in the pathogenesis of AD using a Tg2576 mouse model of AD. These mice express the Swedish mutant of amyloid precursor protein in the brains and have amyloid plaques consisting of Aβ increasing in an age-dependent manner (Hsiao *et al.* 1996; Kawarabayashi *et al.* 2001). We found that in the Tg2576 mouse brain the amyloid plaques could activate microglia but not sufficiently to induce IDO expression. We also found that an additional brain inflammation generated systemically, such as a peritoneal challenge with lipopolysaccharide, was required for IDO induction in the activated microglia infiltrating into amyloid plaques (Akimoto *et al.* 2007). In this sense, the microglial cells are 'primed' by Aβ which activates IDO and KP in response to a subsequent brain inflammation. The secondary brain inflammation is likely to be mediated by proinflammatory cytokines including interleukin-1β (IL-1β), IL-6, tumor necrosis factor-α (TNF-α), and interferon-γ (IFN-γ), all able to activate microglia (Basu *et al.* 2002). Increased levels of these cytokines have been found in the brain of Tg2576 mice during such systemic inflammation (Sly *et al.* 2001). We hypothesized here that proinflammatory cytokines might further stimulate the microglia primed by Aβ for the expression of IDO. In this study, we used THP-1 cells (a human monocytic cell line) and human peripheral blood mononuclear cells (PBMC), both of which are commonly used as model for the microglial response to Aβ and proinflammatory cytokines (Giri *et al.* 2003; Wilkinson *et al.* 2006).

Materials and methods

Materials

Synthetic Aβ peptides (1–40, 1–42, 42–1, and 25–35) were purchased from Peptide Institute Inc. (Osaka, Japan), and prepared as stock solution in dimethyl sulfoxide at a concentration of 4 mM. Human recombinant IL-1β, IL-6, and TNF-α were purchased from Roche Diagnostics, Tokyo, Japan, and human recombinant IFN-γ was purchased from Sigma (St Louis, MO, USA). One unit of the biological activity of each cytokine was defined according to the manufacture's instruction. All cytokines were dissolved in phosphate-buffered saline (PBS) containing 0.1% bovine serum albumin and stored at −80°C until use. Anti-human IDO monoclonal antibody (mAb) was purified from culture medium of a hybridoma clone established by Takikawa *et al.* (1988). Histofine® Simple Stain MAX PO, a horseradish peroxidase-conjugated secondary antibody for immunoblotting, was purchased from NICHIREI (Tokyo, Japan). Anti-TNF-α mAb (IgG_1) was obtained from R & D Systems (Tokyo, Japan). Control mouse IgG_1 was a product of Sigma. THP-1 cells, a human acute monocytic leukemia cell line (Tsuchiya *et al.* 1980), were obtained from Health Science Research Resources Bank (Osaka, Japan).

Cell culture and cellular assay

THP-1 cells were maintained in RPMI-1640 (Sigma, St Louis, MO, USA) containing 10% heat-inactivated fetal calf serum at 37°C in 5% CO_2 and 95% air. The cells used in this study were between passages 12 and 15. Human PBMC were isolated from blood of healthy volunteers with Ficoll-paque PLUS solution (GE Healthcare Life Sciences, Tokyo, Japan), and separated from lymphocytes on the basis of plastic adherence as described by Guillemin *et al.* (2003). PBMC were cultured in Dulbecco's modified Eagle's medium (Sigma) containing 20% heat-inactivated fetal calf serum and 10% heat-inactivated human AB serum at 37°C in 5% CO_2 and 95% air. Before cellular assay, cells were washed once with a serum-free AIM-V medium (Invitrogen, Carlsbad, CA, USA), re-suspended in the AIM-V, and plated in culture plate. Kynurenine (Kyn) concentration in culture medium was determined after deproteinization with trichloroacetic acid at a final concentration of 5% with a Shimadzu Prominence® HPLC system (Kyoto, Japan) equipped with an Insertsil® reverse phased column (4.6 mm x 15 cm; GL Science,

© 2009 The Authors
Journal Compilation © 2009 International Society for Neurochemistry,

Tokyo, Japan). The mobile phase was 10% methanol/10 mM ammonium acetate and Kyn was detected by absorbance at 360 nm. Phase contrast photomicrographs of THP-1 cells (Fig. 2) were taken using an Olympus IX70 inverted microscope (Tokyo, Japan) equipped with a Leica DFC290 digital camera (Wetzlar, Germany). The study with PBMC from blood of healthy volunteers was approved by the human ethical committee of the National Center for Geriatrics and Gerontology and all participants signed informed consent.

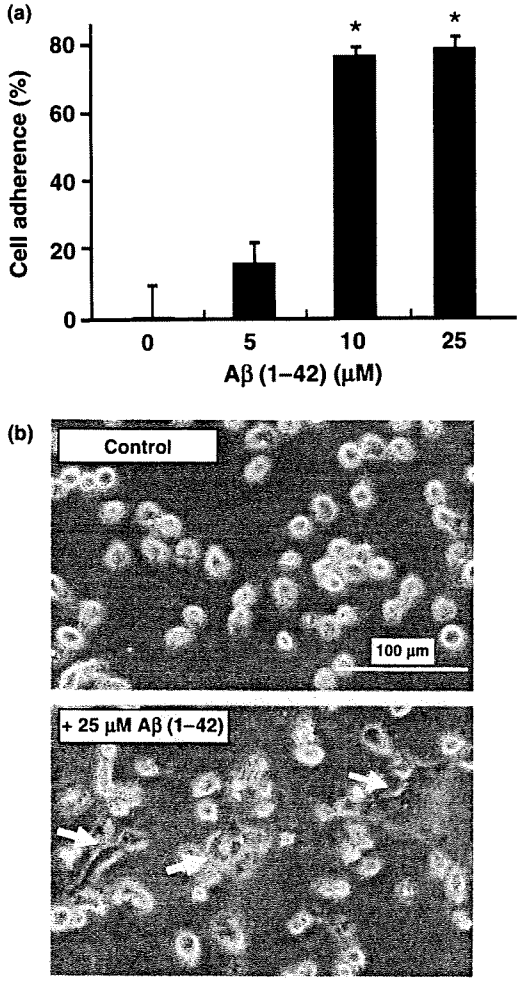

Fig. 2 Increase in adherent activity and change in morphology of THP-1 cells treated with Aβ (1–42). (a) Adherent activity of THP-1 cells treated with Aβ (1–42). THP-1 cells (1×10^5 cells) suspended in 1.0 mL of the AIM-V medium in a 24-well plate were treated with indicated concentrations of Aβ. After 24 h, non-adherent cells were gently collected from the culture plate by pipetting and counted with a hemocytometer under a microscope. $^*p < 0.01$ compared with the control cells treated with the peptide vehicle (0.63% of dimethylsulfoxide at a final concentration). (b) Phase contrast microphotographs of THP-1 cells treated with the peptide vehicle (upper) or 25μM Aβ (1–42) (lower) for 24 h. Arrows indicate typical ameboid spread cells. Scale bar: 100 μm. Magnification: 200×.

Assay of IDO activity

Indoleamine 2,3-dioxygenase activity in cells was assayed as described previously (Takikawa *et al.* 1988). Cultured cells were collected by trypsinization or pipetting, washed with twice with cold PBS, and disrupted by sonication for 30 s in cold PBS containing Complete proteinase inhibitor cocktail (Roche Diagnostics). The cellular homogenate was then centrifuged at 15 000 *g* for 10 min for 5 min at 4°C and the supernatant (cellular extract) was used as the enzyme source. The reaction mixture (200 μL) contained 50 mM potassium phosphate buffer (pH 6.5), 20 mM ascorbate, 10 mM methylene blue, 100 mg/mL catalase, 400 mM tryptophan, and the cellular extract. The reaction at 37°C was started by the addition of tryptophan and terminated after 60 min with trichloroacetic acid at a final concentration of 5% and further incubated at 50°C to hydrolyze *N*-formlylkynurenine to Kyn. After centrifugation at 15 000 *g* for 5 min at 25°C, Kyn in the supernatant was measured by HPLC as described above. Under this condition, the production of Kyn form tryptophan increased linearly for up to 90 min. Protein of the cellular extract was determined using a bicinchoninic acid protein assay kit (Pierce, Rockford, IL, USA) with bovine serum albumin as standard.

Immunoblotting

Cells were lysed in the lysis buffer (1% Triton X-100 in PBS containing Complete proteinase inhibitor cocktail) for 30 min on ice. After insolubles were removed from the lysate by centrifugation for 10 min at 10 000 *g* at 4°C, protein concentration of the cell lysate was measured by bicinchoninic acid protein assay kit (Pierce). Aliquots containing 10 μg of protein were resolved by 12.5% sodium dodecyl sulfate–polyacrylamide gel electrophoresis and transferred onto Immobilon-P transfer membranes (Millipore Corporation, Bedford, MA, USA). The membranes were sequentially reacted with blocking solution, primary antibody (1 : 10000), and the secondary antibody (1 : 500) for 1 h at 25°C. Blots were detected by ECL plus (GE Healthcare). Band intensities were quantified using Scion image software (Scion Corp., Frederic, MD, USA).

RNA isolation and quantitative RT-PCR

Total RNA were isolated from THP-1 cells using a standard method with Trizol® reagent (Invitrogen), and reverse-transcribed by SuperScript®First-Strand Synthesis System for RT-PCR (Invitrogen). Quantitative RT-PCR (qRT-PCR) was performed using SYBER premix EX *taq* (Takara Bio Inc., Otsu, Japan) with a thermal cycler Dice RealTime System TP800 (Takara Bio Inc) according to the manufacturer's instruction. Comparison of IDO expression among the different experimental groups was performed with relative amount of IDO mRNA normalized to glyceraldehyde-3-phosphate dehydrogenase mRNA as an internal standard. The sequences of primers were 5′-TCTTCTCA- TTTCGTGATGGAG-ACTG-3′ and 5′-AAAGTGTCCCGTTCTTGCATTTG-3′ for IDO, and 5′-GCACCGTCAAGGCTGAGAAC-3′ and 5′-TGGTGAA-GACGCCAGTGGA- 3′ for glyceraldehyde-3-phosphate dehydrogenase.

Antibody neutralization assay

Anti-human TNF-α mAb or control isotype mouse IgG (IgG_1) was added into THP-1 cell culture at 1 μg/mL with Aβ (1–42). After

© 2009 The Authors

culture for 24 h, IFN-γ was added to the culture and further incubated for 24 h. The concentration of Kyn in culture medium was determined by HPLC as described above.

Statistical analysis

Each value in all figures represents the mean ± SD of the three separate experiments. All data were analyzed by ANOVA. If a significant difference was identified, multiple comparisons were adjusted using the Scheffe's test. $p < 0.01$ was regarded as statistically significant.

Results

Activation of THP-1 cells by Aβ (1–42)

To mimic the *in vivo* situation in which microglia surrounding amyloid plaques consisting of Aβ in Tg2576 mice are activated by continuous contact with Aβ, we added Aβ to culture of THP-1 cells and examined the cell adherence to plastic plate as cell adherence is a hallmark of monocyte/macrophage activation (Kamal and Harold 1998). After treatment with Aβ (1–42) for 24 h, THP-1 cells became adherent in a dose-dependent manner; at 5 μM of Aβ (1–42), about 20% of the cells attached to the plate and at over 10 μM, most of the cells were adherent (Fig. 2a). This effect was observed only for Aβ (1–42) but not Aβ (1–40) or Aβ 25–35 even at 25 μM (data not shown). The negative control peptide Aβ (42–1) at 25 μM was also totally inactive (data not shown). The activation of THP-1 cells by Aβ (1–42) was associated with marked changes in morphology from round shape to ameboid spread shape (Fig. 2b) which is a characteristic morphological feature of reactive monocytes/macrophages (Kamal and Harold 1998).

Effect of various proinflammatory cytokines on the Kyn production in THP-1 cells pre-treated with Aβ (1–42)

To examine if the adherence of the THP-1 cells generated by Aβ (1–42) induces IDO and activate the KP, we measured the level of tryptophan metabolite Kyn in the culture medium using HPLC. We found that the increase in the level of Kyn after stimulation with Aβ (1–42) for 24 h was very low (0.1–0.2 μM), indicating that IDO was hardly activated. This was confirmed by immunoblotting of IDO protein and qRT-PCR for IDO mRNA as described below. Then we tested our hypothesis that a secondary stimulation by proinflammatory cytokines may induce the activation of KP in the reactive THP-1 cells. To this end, we first pre-treated the THP-1 cells with Aβ (1–42) at 25 μM for 24 h, then added proinflammatory cytokines, IL-1β, IL-6, TNF-α, or IFN-γ to the culture at 100 U/mL, and determined the levels of Kyn in the culture medium 24 h after the addition of cytokine. Of these cytokines, only IFN-γ enhanced markedly the production of Kyn from the reactive THP-1 cells (Fig. 3). This enhancement was more prominent at higher concentrations of IFN-γ and was also dependent on the concentration of Aβ (1–42)

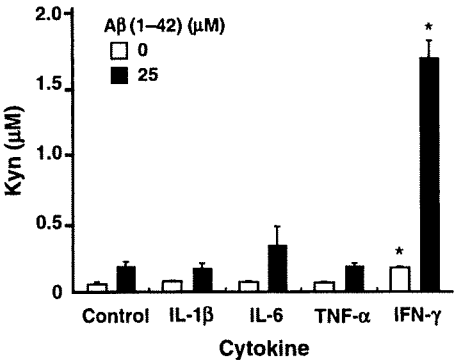

Fig. 3 Production of Kyn in THP-1 cells treated with Aβ (1–42) and proinflammatory cytokines. THP-1 cells (5×10^4 cells) suspended in 0.2 mL of the AIM-V medium in a 96-well plate were treated with the peptide vehicle or 25 μM Aβ (1–42) for 24 h, and then further cultured for 24 h with proinflammatory cytokines at 100 U/mL or the cytokine vehicle (0.1% bovine serum albumin in PBS) (control). The levels of Kyn in the culture medium were measured after additional 24 h culture. □, the peptide vehicle; ■, 25 μM Aβ (1–42). *$p < 0.01$ compared with each control treated with or without the Aβ.

(Fig. 4). It is worth noting that the dose-dependency of Aβ (1–42) for the Kyn production almost coincided with that for the conversion of THP-1 cells to the adherent reactive cells (Fig. 2). Pre-treatment with Aβ (1–40) or Aβ (25–35) at 5–50 μM neither induced THP-1 cells to become adherent reactive cells nor activate the KP by the secondary stimulation with IFN-γ (10–1000 U/mL) (data not shown). Taken together these results indicated that changes in cell morphology induced by Aβ (1–42) were closely associated with the activation of the KP by IFN-γ.

Optimization of pre-treatment with Aβ (1–42) for the IFN-γ-mediated activation of KP in THP-1 cells

We determined the optimal duration of the pre-treatment with Aβ (1–42) required for the IFN-γ-mediated activation of KP in THP-1 cells. Lack of pre-treatment and pre-treatment for 12 h with the addition of Aβ did not induce any KP activation by IFN-γ. A minimum of 24 h pre-treatment was necessary to lead to a significant activation by IFN-γ (Fig. 5a). We also found that the pre-treatment with Aβ (1–42) for 24 h caused a long-term sustained activation of KP by IFN-γ for up to 72 h (Fig. 5b). These results demonstrated that pre-treatment of THP-1 cells with Aβ (1–42) for more than 24 h was required to the subsequent higher KP activation by IFN-γ.

Analysis of IDO expression in THP-1 cells stimulated by Aβ (1–42) and IFN-γ

The levels of Kyn in culture medium of various cells are closely related to those of IDO expressed by the cells (Takikawa *et al.* 1988). Therefore, we analyzed the changes in IDO expression in THP-1 cells stimulated with the

© 2009 The Authors
Journal Compilation © 2009 International Society for Neurochemistry,

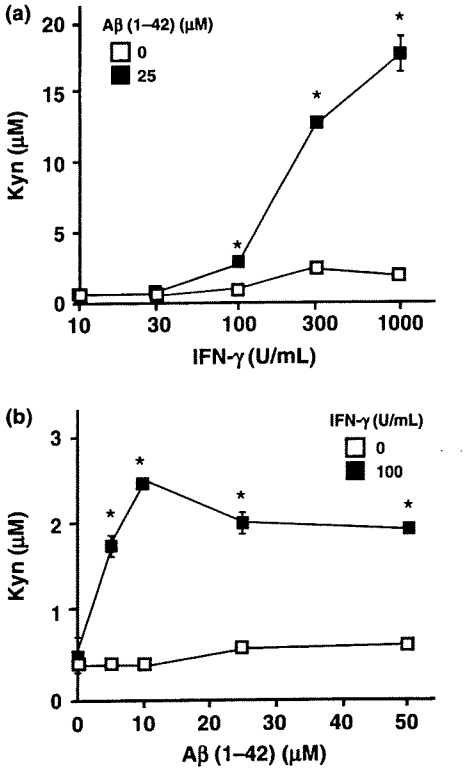

Fig. 4 Production of Kyn in THP-1 cells stimulated with the combination of Aβ and IFN-γ. (a) The dose-dependency of IFN-γ. THP-1 cells (5×10^4 cells) suspended in 0.2 mL of the AIM-V medium in a 96-well plate were first treated with (■)or without (□) 25 μM Aβ (1–42) for 24 h and stimulated with indicated concentrations of IFN-γ for additional 24 h. The levels of Kyn in the culture medium were measured after the stimulation with IFN-γ. □, peptide vehicle; ■, +Aβ 1–42 (25 μM). *$p < 0.01$ compared with the values obtained with the peptide vehicle. (b) The dose-dependency of Aβ (1–42). THP-1 cells (5×10^4 cells) suspended in 0.2 mL of the AIM-V medium in a 96-well plate were first treated with indicated concentrations of Aβ (1–42) for 24 h and further stimulated with 100 U/mL of IFN-γ (■) or the cytokine vehicle (0.1% BSA in PBS) (□) for additional 24 h. The levels of Kyn in the culture medium were measured after the secondary stimulation. □, cytokine vehicle; ■, IFN-γ (100 U/mL). *$p < 0.01$ compared with the values obtained with the cytokine vehicle.

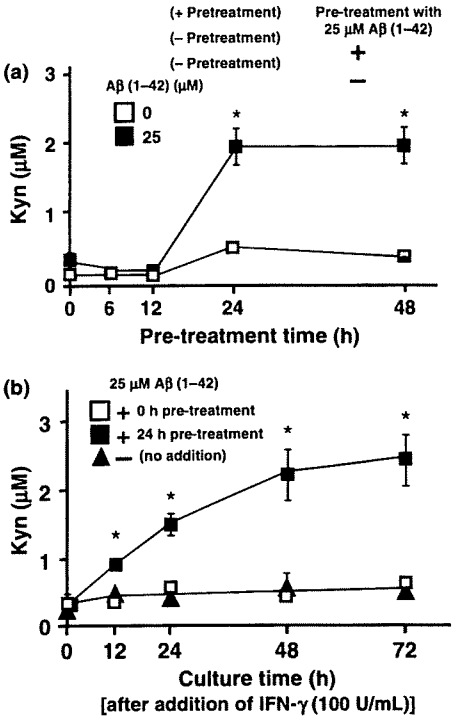

Fig. 5 Optimum duration of the Aβ (1–42) pre-treatment for the activation of KP by IFN-γ in THP-1 cells and the time course of the production of Kyn in the reactive THP-1 cells stimulated with IFN-γ. (a) Effect of pre-treatment time with Aβ (1–42) for the production of Kyn by the subsequent stimulation with IFN-γ in THP-1 cells. THP-1 cells (5×10^4 cells) suspended in 0.2 mL of the AIM-V medium in a 96-well plate were cultured with 25 μM Aβ (1–42) (■) or without the peptide (i.e., with the peptide vehicle) (□). At indicated culture periods (6, 12, 24, and 48 h), IFN-γ (100 U/mL) was added to the cultures and the levels of Kyn in culture medium were measured after additional 24 h culture. □, peptide vehicle; ■, +25 μM Aβ (1–42). *$p < 0.01$ compared with the values obtained without the pre-treatment with the Aβ. (b) The time course of the production of Kyn in the THP-1 cells stimulated with the combination of Aβ (1–42) and IFN-γ. THP-1 cells (5×10^4 cells) suspended in 0.2 mL of the AIM-V medium in a 96-well plate were pre-treated with 25 μM Aβ (1-42) for 24 h and further cultured with 100 U/mL IFN-γ for up to 72 h. The time course of Kyn production in the cultures after the addition of IFN-γ was depicted with ■. Those of the cultures stimulated simultaneously with 25 μM Aβ (1–42) and 100 U/mL IFN-γ or stimulated with 100 U/mL IFN-γ alone after pre-treatment of the peptide vehicle for 24 h were indicated with □ and ▲, respectively. *$p < 0.01$ compared with the values obtained without culture with IFN-γ.

combination of Aβ (1–42) and IFN-γ. IDO mRNA was very weakly expressed in THP-1 cells when cultured without any stimulation. This expression increased by 7.2 ± 1.7-fold upon stimulation with 25 μM Aβ (1–42) alone and was strongly elevated by 3156 ± 488.8-fold in combination with IFN-γ at 100 U/mL (Fig. 6a). Stimulation with IFN-γ alone without pre-treatment with Aβ (1–42) resulted in small increase of 65 ± 5.2-fold in mRNA levels; (Fig. 6a). In accordance with these qRT-PCR results, both IDO enzyme activity (Fig. 6b) and the level of IDO protein (Fig. 6c) were markedly elevated by the sequential stimulation with Aβ and IFN-γ. Taken together, these results showed that KP activation in THP-1 cells by Aβ (1–42) and IFN-γ was associated with an increase in IDO transcript and functional IDO protein.

Analysis of IDO expression in PBMC stimulated with Aβ (1–42) and IFN-γ

It could be possible that the above-mentioned KP activation may be the unique property of THP-1 cells acquired during immortalization. Therefore, we tested if the similar

© 2009 The Authors
Journal Compilation © 2009 International Society for Neurochemistry,

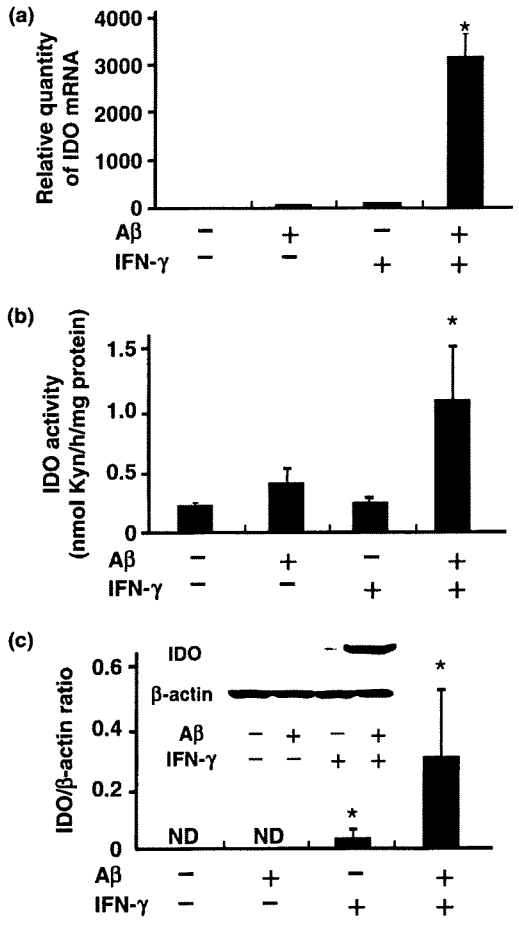

Fig. 6 Analysis of the expression of IDO in THP-1 treated with the combination of Aβ (1–42) and IFN-γ. THP-1 cells (1×10^5 cells) suspended in 1.0 mL of the AIM-V medium in a 24-well plate were analyzed after pre-treatment with or without 25 μM Aβ (1–42) for 24 h and further stimulation with or without 100 U/mL IFN-γ for 24 h. (a) qRT-PCR of IDO mRNA. The levels of IDO mRNA were normalized with those of glyceraldehyde-3-phosphate dehydrogenase (GAPDH) mRNA and expressed as relative quantity to that of the control (the control value: 1) without stimulation with 25 μM Aβ (1–42) nor 100 U/mL IFN-γ. (b) IDO enzyme activity. (c) Immunoblot analysis of IDO protein. The band intensities of IDO were normalized with those of β-actin. *$p < 0.01$ compared with others. ND, not detectable.

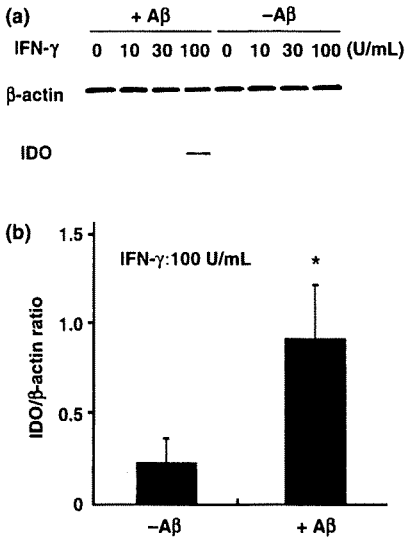

Fig. 7 Analysis of IDO expression in PBMC treated with Aβ (1–42) and IFN-γ. (a) Immunoblotting of IDO in PBMC. PBMC (1×10^5 cells) suspended in 1.0 mL of AIM-V medium and cultured in a 24-well plate with the peptide vehicle or 25 μM Aβ (1–42) for 24 h and further stimulated with indicated concentrations of IFN-γ for 24 h. IDO expression in PBMC was analyzed by immunoblotting after stimulation with IFN-γ. (b) Quantitative analysis of the immunoblots. The band intensities obtained with 100 U/mL IFN-γ were normalized with those of β-actin. *$p < 0.01$ compared with the value obtained with the peptide vehicle (−Aβ).

combinational effects of Aβ (1–42) and IFN-γ could also induce IDO in primary cultures of human peripheral blood mononuclear cells (PBMC). PBMC were first pre-treated with 25 μM Aβ (1–42) for 24 h, then stimulated with different concentrations of IFN-γ for another 24 h, and analyzed by immunoblotting. Similar to THP-1 cells, IDO expression in PBMC was undetectable without any stimulation but weakly induced by IFN-γ alone (Fig. 7a). However, with the Aβ (1–42) pre-treatment, IDO expression was greatly enhanced by IFN-γ in a dose-dependent manner (Fig. 7a). In fact, the pre-treatment increased IDO protein level by about fourfold with 100 U/mL IFN-γ (Fig. 7b), which was comparable with results with THP-1 cells (Fig. 6c). Thus, the high IDO induction by the sequential stimulation with Aβ (1–42) and IFN-γ was well similar between human monocytic cell line THP-1 cells and human primary PBMC.

Involvement of TNF-α in KP activation by Aβ (1–42) and IFN-γ

We previously demonstrated that IDO is induced by IFN-γ in many different cell types (Takikawa *et al.* 1988), and other showed that this induction could be enhanced by TNF-α in macrophages and epithelial cells (Currier *et al.* 2000; Robinson *et al.* 2003). Other studies also reported that TNF-α secretion by microglial cells was induced by a combination of Aβ (1–42) and IFN-γ (Meda *et al.* 1995; Klegeris *et al.* 1997). We therefore hypothesized that an autocrine stimulation by TNF-α may be involved in KP activation in THP-1 cells by the sequential treatment with Aβ (1–42) and IFN-γ. To test this hypothesis, we stimulated THP-1 cells with Aβ (1–42) and IFN-γ in the presence of anti-TNF-α mAb at 1 μg/mL, which was able to neutralize as much as 100 U/mL of TNF-α. The anti-TNF-α mAb inhibited the Kyn production by more than 60% (39.1 ± 8.7%) whereas the control isotype IgG_1 at 1 μg/mL

© 2009 The Authors
Journal Compilation © 2009 International Society for Neurochemistry,

Table 1 Effect of anti-TNF-α mAb on the production of Kyn in THP-1 cells treated with the combination of Aβ (1–42) and IFN-γ

	Kyn (μM)	Percent of control
Control	2.3 ± 0.2	100.0
+Anti-TNF-α (1 μg/mL)	0.9 ± 0.2	39.1 ± 8.7*
+IgG1 (1 μg/mL)	2.2 ± 0.1	95.6 ± 4.3

TNF-α, tumor necrosis factor α; Kyn, kynurenine.
THP-1 cells (5×10^4 cells) suspended in 0.2 mL of AIM-V medium were cultured in a 96-well plate with 25 μM Aβ (1–42) in the presence of anti-human TNF-α mAb (IgG_1) or control isotype IgG_1 at 1 μg/mL for 24 h. Control cells were cultured with 25 μM Aβ (1–42) alone. Then IFN-γ was added to the cultures at 100 U/mL and cultured for another 24 h. Kyn was measured in culture supernatants after the additional 24 h culture.
*$p < 0.01$ compared with others.

was totally ineffective (Table 1). These results indicated that an autocrine TNF-α was significantly involved in the KP activation in THP-1 cells.

Discussion

In this study, we tested our hypothesis that activated microglia surrounding amyloid plaques consisting of Aβ are 'primed' for the activation of KP in response to the additional stimulation by proinflammatory cytokines. We used THP-1 cells and human primary PBMC as models for microglia, and found that both monocytic cell types pre-treated with Aβ (1–42), one of the main components of amyloid plaques, become highly responsive to a secondary stimulation with the proinflammatory cytokine IFN-γ and markedly activate the KP through induction of IDO. Only the combination of Aβ (1–42) and IFN-γ was able to activate the KP whereas Aβ (1–40) or Aβ (25–35) and other major proinflammatory cytokines including IL-1β, TNF-α, or IL-6 were not (Fig. 3), although an autocrine TNF-α was partly involved in the induction of IDO (Table 1). However, the combined concomitant stimulation of THP-1 cells with Aβ (1–42) and IFN-γ did not activate the KP. We showed that a pre-treatment with Aβ (1–42) for at least 24 h was prerequisite for the secondary stimulation with IFN-γ to be effective on the KP activation (Fig. 5). This pre-treatment with Aβ lead to a cellular activation as shown by the morphological change and enhanced adhesiveness (Fig. 2). This activation by Aβ (1–42) alone, however, was not sufficient to switch on the cellular machinery involved in IDO induction (Fig. 4). Thus, our *in vitro* model further supported our hypothesis that the microglia receiving a chronic stimulation by amyloid plaques consisting of Aβ (1–42) are 'primed' for the activation of KP by the induction of IDO in a response to the proinflammatory cytokine IFN-γ.

Both THP-1 cells primed with Aβ (1–42) and PBMC differentiated by granulocyte macrophage-colony stimulating factor (GM-CSF) have a similar response in term of KP activation by IFN-γ (Jansen and Reinhard 1999). However, PBMC required longer time of culture (3 to 7 days) with GM-CSF to adopt a reactive state in response to the IFN. These differentiated cells did not exhibit such strong morphological changes and adhesiveness as we found with THP-1 cells after a short (24 h) pre-treatment with Aβ (1–42) (Fig. 2). Therefore, the cellular changes induced by GM-CSF appear to be different from those with Aβ 'priming'.

What is the relevance of these present findings to the pathogenesis of AD? It is known that systemic inflammatory infection is the risk factor for AD progression (Holmes *et al.* 2003) and that similar systemic inflammation caused by an intraperitoneal injection of lipopolysaccharide increased proinflammatory cytokine production including IFN-γ in the mouse brain (Pitossi *et al.* 1997). Level of IFN-γ in the mouse brain increased with aging (Frank *et al.* 2006; Kumagai *et al.* 2007), which represented the major risk factor for AD (Evans *et al.* 1989; Hebert *et al.* 2003). On the other hand, it has been recently reported that IFN-γ can be produced by mouse microglia when stimulated with IL-18 (Kawanokuchi *et al.* 2006) and that expression of IL-18 is elevated in microglia, astrocytes, and neurons within the AD brains (Ojala *et al.* 2009). Under stress conditions, IL-18 was also involved in the activation of murine microglia (Sugama *et al.* 2007), which accelerated learning and memory impairment and worsened the amyloid pathology in the mouse models of AD (Dong *et al.* 2004; Jeong *et al.* 2006). Therefore, under neuroinflammatory conditions (infection, aging, and stress) associated with the accelerating progression in both human AD or the AD-like pathology of the mouse models, 'primed' microglia surrounding amyloid plaques appear to be activated by IFN-γ to induce IDO and to produce neurotoxic QUIN, thereby promoting the neurodegeneration. In the rat brain QUIN neurotoxicity was greatly enhanced by proinflammatory cytokine IL-1β (Stone and Behan 2007). This neurotoxic combination is likely to reach neurons around amyloid plagues in human AD brains, as production of both QUIN and IL-1β was increased in activated microglia attacking senile plaques (Griffin *et al.* 1989; Guillemin *et al.* 2005b). Thus, our findings may explain some part of the molecular mechanisms underlying the accelerated neurodegeneration by risk factors known to enhance inflammation in the AD brain.

Aβ (1–40) and Aβ (1–42) are the major components of amyloid plaques (Gravina *et al.* 1995; Kawarabayashi *et al.* 2001). However, considerable circumstantial evidence suggests that Aβ (1–42) rather than Aβ (1–40) is the critical molecule involved in the pathogenesis of AD (Jarrett *et al.* 1993; Iwatsubo *et al.* 1994; Gravina *et al.* 1995; McGowan *et al.* 2005). In fact, even at lower concentrations Aβ (1–42) was significantly more toxic to cultured neurons compared with Aβ (1–40) (Drouet *et al.* 2000; Dahlgren *et al.* 2002). Aβ (1–42) can form soluble oligomeric structures, insoluble

© 2009 The Authors
Journal Compilation © 2009 International Society for Neurochemistry,

fibrils, and highly aggregated form of the fibrils at lower concentrations and higher rates compared with Aβ (1–40) or any other Aβ variants (Burdick *et al.* 1992; Jarrett *et al.* 1993). These unique properties of Aβ (1–42) may be responsible for the specificity for the priming effect on the induction of IDO in THP-1 cells.

Several surface receptors expressed in monocytic cells including microglia have been reported to interact with Aβ fibrils; among them the scavenger receptor complex consisting of class A scavenger receptor, CD36, α6/β1-integlin, and CD47 (El Khoury *et al.* 1996; Wilkinson *et al.* 2006), the receptor for advanced glycation end products (Yan *et al.* 1996), and Toll-like receptors 2 and 4 (Chen *et al.* 2006; Richard *et al.* 2008; Udan *et al.* 2008). Our preliminary data (not shown) suggested that the scavenger receptor complex was not involved in the priming effect of Aβ (1–42) because the antagonist for the receptor complex, 4N1K peptide at up to 300 μM (Wilkinson *et al.* 2006) did not suppress the induction of IDO. Moreover, the phagocytosis of Aβ fibrils was not required for the effect of Aβ (1–42) as treatment with an inhibitor of phagocytosis, cytochalasin D (3 μM) (Sulahian *et al.* 2008) did not inhibit the enzyme induction (data not shown). The possible involvement of receptor for advanced glycation or Toll-like receptor 2/4 in the priming effect of Aβ (1–42) is currently under investigation.

It is generally accepted that inflammation-mediated neurotoxicity in neurodegenerative disease including AD can occur as a consequence of microglial overactivation (Perry *et al.* 2003; Block *et al.* 2007). This concept is based on the fact that such over-activated microglia can generate neurotoxic products including reactive oxygen species and proinflammatory cytokines (Cunningham *et al.* 2005; Block *et al.* 2007). In addition to these neurotoxic compounds, we previously demonstrated that activated microglia associated with amyloid plaques in human AD brains produced neurotoxic amounts of QUIN (Guillemin *et al.* 2005a, 2007). Based on our previous *in vivo* findings in Tg2576 mice and our present *in vitro* data with models of microglia, we concluded that the microglia producing QUIN in AD brains were over-activated by the combination of the chronic exposure to amyloid peptides, and more particularly Aβ (1–42), and the secondary inflammatory cytokine, IFN-γ. Several drugs that block the KP are currently under therapeutic investigation by our laboratory and others. Targeting IDO or other KP enzymes with specific inhibitors would lead to a decrease in QUIN production and may therefore bring new therapeutic strategies for AD.

Acknowledgment

This work was supported by the Program for Promotion of Fundamental Studies in Health Sciences of the National Institute of Biomedical Innovation (NIBIO).

References

Akimoto H., Yamada A. and Takikawa O. (2007) Up-regulation of the brain indoleamine 2,3-dioxygenase activity in a mouse model of Alzheimer's disease by systemic endotoxin challenge, in *International Congress Series* (Takai K., ed.), Vol. 1304, pp. 357–361. Elsevier Science B. V., Amsterdam.

Basu A., Krady J. K., Enterline J. R. and Levison S. W. (2002) Transforming growth factor beta1 prevents IL-1beta-induced microglial activation, whereas TNF alpha- and IL-6-stimulated activation are not antagonized. *Glia* **40**, 109–120.

Block M. L., Zecca L. and Hong J. S. (2007) Microglia-mediated neurotoxicity: uncovering the molecular mechanisms. *Nat. Rev. Neurosci.* **8**, 57–69.

Burdick D., Soreghan B., Kwon M., Kosmoski J., Knauer M., Henschen A., Yates J., Cotman C. and Glabe C. (1992) Assembly and aggregation properties of synthetic Alzheimer's A4/beta amyloid peptide analogs. *J. Biol. Chem.* **267**, 546–554.

Chen K., Iribarren P., Hu J. *et al.* (2006) Activation of Toll-like receptor 2 on microglia promotes cell uptake of Alzheimer disease-associated amyloid β peptide. *J. Biol. Chem.* **281**, 3651–3659.

Cunningham C., Wilcockson D. C., Campion S., Lunnon K. and Perry V. H. (2005) Central and systemic endotoxin challenges exacerbate the local inflammatory response and increase neuronal death during chronic neurodegeneration. *J. Neurosci.* **25**, 9275–9284.

Currier A. R., Ziegler M. H., Riley M. M. *et al.* (2000) Tumor necrosis factor-alpha and lipopolysaccharide enhance interferon-induced antichlamydal indoleamine dioxygenase activity independently. *J. Interferon Cytokine Res.* **20**, 369–376.

Dahlgren K. N., Manelli A. M., Stine W. B. Jr, Baker L. K., Krafft G. A. and LaDu M. J. (2002) Oligomeric and fibrillar species of amyloid-beta peptides differentially affect neuronal viability. *J. Biol. Chem.* **277**, 32046–32053.

Dong H., Goico B. and Martin M. (2004) Modulation of hippocampal cell proliferation, memory, and amyloid plaque deposition in APPsw (Tg2576) mutant mice by isolation stress. *Neuroscience* **127**, 601–609.

Drouet B., Pinçon-Raymond M., Chambaz J. and Pillot T. (2000) Molecular basis of Alzheimer's disease. *Cell. Mol. Life Sci.* **57**, 705–715.

El Khoury J., Hickman S. E., Thomas C. A. *et al.* (1996) Scavenger receptor-mediated adhesion of microglia to beta-amyloid fibrils. *Nature* **382**, 716–719.

Evans D. A., Funkenstein H. H., Albert M. S., Scherr P. A., Cook N. R., Chown M. J., Hebert L. E., Hennekens C. H. and Taylor J. O. (1989) Prevalence of Alzheimer's disease in a community population of older persons. Higher than previously reported. *JAMA* **262**, 2551–2556.

Frank M. G., Barrientos R. M., Biedenkapp J. C. *et al.* (2006) mRNA up-regulation of MHC II and pivotal pro-inflammatory genes in normal brain aging. *Neurobiol. Aging* **27**, 717–722.

Giri R. K., Selvaraj S. K. and Kalra V. K. (2003) Amyloid peptide-induced cytokine and chemokine expression in THP-1 monocytes is blocked by small inhibitory RNA duplexes for early growth response-1 messenger RNA. *J. Immunol.* **170**, 5281–5294.

Gravina S. A., Ho L., Eckman C. B., Long K. E., Otvos L. Jr, Younkin L. H., Suzuki N. and Younkin S. G. (1995) Amyloid beta protein (A beta) in Alzheimer's disease brain. Biochemical and immunocytochemical analysis with antibodies specific for forms ending at A beta 40 or A beta 42 (43). *J. Biol. Chem.* **270**, 7013–7016.

Griffin W. S., Stanley L. C., Ling C., White L., MacLeod V., Perrot L. J., White C. L. 3rd and Araoz C. (1989) Brain interleukin 1 and S-100 immunoreactivity are elevated in Down syndrome and Alzheimer disease. *Proc. Natl Acad. Sci. USA* **86**, 7611–7615.

© 2009 The Authors
Journal Compilation © 2009 International Society for Neurochemistry,

Guillemin G. J., Smythe G., Veas L., Takikawa O. and Brew B. J. (2003) Aβ1-42 induces production of quinolinic acid by human macrophages and microglia. *NeuroReport* **14**, 2311–2315.

Guillemin G. J., Meininger V. and Brew B. J. (2005a) Implications for the kynurenine pathway and quinolinic acid in amyotrophic lateral sclerosis. *Neurodegener. Dis.* **2**, 166–176.

Guillemin G. J., Brew B. J., Noonan C. E., Takikawa O. and Cullen K. M. (2005b) Indoleamine 2,3 dioxygenase and quinolinic acid immunoreactivity in Alzheimer's disease hippocampus. *Neuropathol. Appl. Neurobiol.* **31**, 340–395.

Guillemin G. J., Brew B. J., Noonan C. E., Knight T. G., Smythe G. A. and Cullen K. M.. (2007) Mass spectrometric detection of quinolinic acid in microdissected Alzheimer's disease plaques, in *International Congress Series* (Takai K., ed.), Vol. 1304, pp. 404–408. Elsevier Science B. V., Amsterdam.

Hebert L. E., Scherr P. A., Bienias J. L., Bennett D. A. and Evans D. A. (2003) Alzheimer disease in the US population: prevalence estimates using the 2000 census. *Arch. Neurol.* **60**, 1119–1122.

Heyes M. P., Saito K., Crowley J. S., Davis L. E., Demitrack M. A., Der M. and Markey S. P. (1992) Quinolinic acid and kynurenine pathway metabolism in inflammatory and non-inflammatory neurological disease. *Brain* **115**, 1249–1273.

Holmes C., El-Okl M., Williams A. L., Cunningham C., Wilcockson D. and Perry V. H. (2003) Systemic infection, interleukin 1beta, and cognitive decline in Alzheimer's disease. *J. Neurol. Neurosurg. Psychiatry* **74**, 788–789.

Hsiao K., Chapman P., Nilsen S., Eckman C., Harigaya Y., Younkin S., Yang F. and Cole G. (1996) Correlative memory deficits, Abeta elevation, and amyloid plaques in transgenic mice. *Science* **274**, 99–102.

Iwatsubo T., Odaka A., Suzuki N., Mizusawa H., Nukina N. and Ihara Y. (1994) Visualization of A beta 42(43) and A beta 40 in senile plaques with end-specific A beta monoclonals: evidence that an initially deposited species is A beta 42(43). *Neuron* **13**, 45–53.

Jansen M. and Reinhard J. F. Jr (1999) Interferon response heterogeneity: activation of a pro-inflammatory response by interferon alpha and beta. A possible basis for diverse responses to interferon beta in MS. *J. Leukoc. Biol.* **65**, 439–443.

Jarrett J. T., Berger E. P. and Lansbury P. T. Jr (1993) The carboxy terminus of the beta amyloid protein is critical for the seeding of amyloid formation: implications for the pathogenesis of Alzheimer's disease. *Biochemistry* **32**, 4693–4697.

Jeong Y. H., Park C. H., Yoo J., Shin K. Y., Ahn S. M., Kim H. S., Lee S. H., Emson P. C. and Suh Y. H. (2006) Chronic stress accelerates learning and memory impairments and increases amyloid deposition in APPV717I-CT100 transgenic mice, an Alzheimer's disease model. *FASEB J.* **20**, 729–731.

Kamal D. S. and Harold I. M. (1998) Thrombin receptor activation inhibits monocyte spreading by induction of Etb receptor-coupled Nitric Oxide release. *J. Immunol.* **161**, 5039–5044.

Kawanokuchi J., Mizuno T., Takeuchi H. *et al.* (2006) Production of interferon-γ by microglia. *Mult. Scler.* **12**, 534–558.

Kawarabayashi T., Younkin L. H., Saido T. C., Shoji M., Ashe K. H. and Younkin S. G. (2001) Age-dependent changes in brain, CSF, and plasma amyloid beta protein in the Tg2576 transgenic mouse model of Alzheimer's disease. *J. Neurosci.* **21**, 372–381.

Klegeris A., Walker D. G. and McGeer P. L. (1997) Interaction of Alzheimer β-amyloid peptide with the human monocytic cell line THP-1 result in a protein kinase C-dependent secretion of tumor necrosis factor-α. *Brain Res.* **747**, 114–121.

Kumagai N., Chiba Y., Hosono M. *et al.* (2007) Involvement of pro-inflammatory cytokines and microglia in an age-associated neurodegeneration model, the SAMP10 mouse. *Brain Res.* **1185**, 75–85.

McGowan E., Pickford F., Kim J. *et al.* (2005) Abeta42 is essential for parenchymal and vascular amyloid deposition in mice. *Neuron* **47**, 191–199.

Meda L., Cassatella M. A., Szendrei G. I. *et al.* (1995) Activation of microglial cells by β-amyloid protein and interferon-γ. *Nature* **374**, 647–650.

Morgan C., Colombres M., Nuñez M. T. *et al.* (2004) Structure and function of amyloid in Alzheimer's disease. *Prog. Neurobiol.* **74**, 323–349.

Moroni F. (1999) Tryptophan metabolism and brain function: focus on kynurenine and other indole metabolites. *Eur. J. Pharmacol.* **375**, 87–100.

Naritsin D. B., Saito K., Markey S. P., Chen C. Y. and Heyes M. P. (1995) Metabolism of L-tryptophan to kynurenate and quinolinate in the central nervous system: effects of 6-chlorotryptophan and 4-chloro-3-hydroxyanthranilate. *J. Neurochem.* **65**, 2217–2226.

Ogawa T., Matson W. R., Beal M. F. *et al.* (1992) Kynurenine pathway abnormalities in Parkinson's disease. *Neurology* **42**, 1702–1706.

Ojala J., Alafuzoff I., Herukka S. K., van Groen T., Tanila H. and Pirttilä T. (2009) Expression of interleukin-18 is increased in the brains of Alzheimer's disease patients. *Neurobiol. Aging* **30**, 198–209.

Pearson S. J. and Reynolds G. P. (1992) Increased brain concentrations of a neurotoxin, 3-hydroxykynurenine, in Huntington's disease. *Neurosci. Lett.* **144**, 199–201.

Perry V. H., Newman T. A. and Cunningham C. (2003) The impact of systemic infection on the progression of neurodegenerative disease. *Nat. Rev. Neurosci.* **4**, 103–112.

Pitossi F., Rey A. D., Kabiersch A. and Besedovsky H. (1997) Induction of cytokine transcripts in the central nervous system and pituitary following peripheral administraton of endotoxin to mice. *J. Neurosci. Res.* **48**, 287–298.

Richard K. L., Filali M., Préfontaine P. and Rivest S. (2008) Toll-Like Receptor 2 acts as a natural innate immune receptor to clear amyloid β_{1-42} and delay the cognitive decline on a mouse model of Alzheimer's disease. *J. Neurosci.* **28**, 5784–5793.

Robinson C. M., Shirey K. A. and Carlin J. M. (2003) Synergistic transcriptional activation indoleamine dioxygenase by IFN-γ and Tumor Necrosis Factor-α. *J. Interferon Cytokine Res.* **23**, 413–421.

Selkoe D. J. (2001) Alzheimer's disease: genes, proteins, and therapy. *Physiol. Rev.* **81**, 741–766.

Sly L. M., Krzesicki R. F., Brashler J. R., Buhl A. E., McKinley D. D., Carter D. B. and Chin J. E. (2001) Endogenous brain cytokine mRNA and inflammatory responses to lipopolysaccharide are elevated in the Tg2576 transgenic mouse model of Alzheimer's disease. *Brain Res. Bull.* **56**, 581–588.

Smith A. J., Stone T. W. and Smith R. A. (2007) Neurotoxicity of tryptophan metabolistes. *Biochem. Soc. Trans.* **35**, 1287–1289.

Stone T. W. and Behan W. M. (2007) Interleukin-1beta but not tumor necrosis factor-alpha potentiates neuronal damage by quinolinic acid: Protection by an adenosine A (2A) receptor antagonist. *J. Neurosci. Res.* **85**, 1077–1085.

Stone T. W., Behan W. M., Jones P. A., Darlington L. G. and Smith R. A. (2001) The role of kynurenines in the production of neuronal death, and the neuroprotective effect of purines. *J. Alzheimers Dis.* **3**, 355–366.

Stoy N., Mackay G. M., Forrest C. M. *et al.* (2005) Tryptophan metabolism and oxidative stress in patients with Huntington's disease. *J. Neurochem.* **93**, 611–623.

Sugama S., Fujuta M., Hashimoto M. and Conti B. (2007) Stress induced morphological microglial activation in the rodent brain: involvement of interleikin-18. *Neuroscience* **146**, 1388–1399.

Sulahian T. H., Imrich A., Deloid G., Winkler A. R. and Kobzik L. (2008) Signaling pathways required for macrophage scavenger

© 2009 The Authors
Journal Compilation © 2009 International Society for Neurochemistry,

receptor-mediated phagocytosis: analysis by scanning cytometry. *Respir. Res.* **9**, 59.

Takikawa O. (2005) Biochemical and medical aspects of the indoleamine 2,3- dioxygenase-initiated L-tryptophan metabolism. *Biochem. Biophys. Res. Commun.* **338**, 12–19.

Takikawa O., Yoshida R., Kido R. and Hayaishi O. (1986) Tryptophan degradation in mice initiated by indoleamine 2,3-dioxygenase. *J. Biol. Chem.* **261**, 3648–3653.

Takikawa O., Kuroiwa T., Yamazaki F. and Kido R. (1988) Mechanism of interferon-gamma action. Characterization of indoleamine 2,3-dioxygenase in cultured human cells induced by interferon-gamma and evaluation of the enzyme-mediated tryptophan degradation in its anticellular activity. *J. Biol. Chem.* **263**, 2041–2048.

Tsuchiya S., Yamabe M., Yamaguchi Y., Kobayashi Y., Konno T. and Tada K. (1980) Establishment and characterization of a human acute monocytic leukemia cell line (THP-1). *Int. J. Cancer*, **26**, 171–176.

Udan M. L. D., Ajit D., Crouse N. R. and Nichols M. R. (2008) Toll-like receptors 2 and 4 mediate Aβ (1-42) activation of the innate immune in a human monocytic cell line. *J. Neurochem.* **104**, 524–533.

Walker D. G., Link J., Lue L. F., Dalsing-Hernandez J. E. and Boyes B. E. (2006) Gene expression changes by amyloid beta peptide-stimulated human postmortem brain microglia identify activation of multiple inflammatory processes. *J. Leukoc. Biol.* **79**, 596–610.

Wilkinson B., Koenigsknecht-Talboo J., Grommes C. *et al.* (2006) Fibrillar β-amyloid-stimulated intracellular signaling cascades require Vav for induction of respiratory burst and phagocytosis in monocytes and microglia. *J. Biol. Chem.* **281**, 20842–20850.

Yan S. D., Chen X., Fu J. *et al.* (1996) RAGE and amyloid-β peptide neurotoxicity in Alzheimer's disease. *Nature* **382**, 685–691.

© 2009 The Authors
Journal Compilation © 2009 International Society for Neurochemistry,

Indoleamine 2,3-Dioxygenase Expression and Regulation in Chronic Periodontitis

Kanokwan Nisapakultorn,* Jittima Makrudthong,† Noppadol Sa-Ard-Iam,* Pimprapa Rerkyen,* Rangsini Mahanonda,* and Osamu Takikawa‡

Background: Indoleamine 2,3-dioxygenase (IDO) is an intracellular tryptophan-oxidizing enzyme with immunosuppressive characteristics. Its expression and regulation in periodontal tissues are unknown. The aim of this study was to determine IDO expression in healthy gingiva and chronic periodontitis lesions. In addition, the effect of inflammatory cytokines and bacterial products on the expression and activity of DOI in human gingival fibroblasts (HGFs) was assessed.

Methods: Human gingival tissue samples were obtained from patients who underwent periodontal surgery. IDO expression in healthy gingiva and periodontitis lesions was determined by immunohistochemistry. HGF cells were treated with interferon-gamma (IFN-γ), interleukin (IL)-1β, tumor necrosis factor-alpha (TNF-α), and lipopolysaccharides from *Porphyromonas gingivalis* (*Pg*LPS). IDO mRNA expression was determined by reverse transcription-polymerase chain reaction. The IDO enzymatic activity was determined by measuring the kynurenine level using a colorimetric method.

Results: In gingival tissues, IDO expression was detected in epithelial cells, fibroblasts, endothelial cells, and inflammatory mononuclear cells. IDO expression was higher in periodontitis lesions than in healthy gingiva. HGFs did not constitutively express IDO. IFN-γ strongly induced IDO expression and activity in HGFs, in a dose-dependent manner. IL-1β, TNF-α, and *Pg*LPS were also able to induce IDO expression in HGF cells. IFN-γ in combination with IL-1β, TNF-α, or *Pg*LPS showed enhanced IDO expression.

Conclusions: IDO was expressed in human gingiva, and the expression was upregulated in chronic periodontitis. The increased IDO expression in periodontitis lesions may be due, in part, to the activation of HGFs by inflammatory cytokines and bacterial products. *J Periodontol 2009;80:114-121.*

KEY WORDS

Fibroblasts; indoleamine 2,3-dioxygenase; inflammation; periodontitis.

* Department of Periodontology, Chulalongkorn University, Bangkok, Thailand.
† Department of General Dentistry, Srinakarinwirot University, Bangkok, Thailand.
‡ National Institute for Longevity Sciences, National Center for Geriatrics and Gerontology, Aichi, Japan.

Indoleamine 2,3-dioxygenase (IDO) is an enzyme that metabolizes the amino acid tryptophan, the least abundant essential amino acid for mammals. The majority of tryptophan is metabolized along the kynurenine pathway, leading to the synthesis of nicotinamide adenine dinucleotide or the complete oxidation of the amino acid.[1] IDO is expressed in many cell types, including monocytes, macrophages, dendritic cells, fibroblasts, epithelial cells, astrocytes, and several cancer cell lines.[1] Early studies showed that IDO was involved in the interferon-gamma (IFN-γ)-mediated host defense to many intracellular pathogens, including *Toxoplasma*,[2] *Chlamydia*,[3] *Mycobacterium*,[4] *Staphylococcus aureus*,[5] cytomegalovirus,[6] and herpes simplex virus.[7] This antimicrobial effect was mainly mediated through IFN-γ–induced IDO expression and activity.

IDO also plays a role in immunoregulation and tolerance induction. Macrophages and dendritic cells expressing IDO can suppress T-cell responses and promote tolerance.[8] IDO-dependent T-cell suppression seems to be mediated by depletion of tryptophan in the microenvironment. Excess tryptophan was able to reverse the inhibition of T cells.[9,10] Toxic metabolites of tryptophan, such as quinolinic acid and 3-hydroxy-anthranilic acid, may also mediate the immunosuppressive effects of IDO.[11-13]

doi: 10.1902/jop.2009.080315

IDO expression is induced by several inflammatory cytokines and immunomodulating agents. IFN-γ is a potent inducer of IDO expression. Interferon-alpha (IFN-α) and -beta (IFN-β) are also able to induce IDO expression, but to a lesser extent.[14] Tumor necrosis factor-alpha (TNF-α), interleukin (IL)-1, and lipopolysaccharide (LPS) also induce IDO expression alone or in combination with IFN-γ.[15,16] Because IDO expression may lead to suppression of T-cell proliferation and function, induction of IDO expression by inflammatory cytokines and immunomodulating agents may limit excessive T-cell activation at local sites of inflammation, thus, serving an anti-inflammatory role.

Various cytokines that regulate IDO expression and activity were detected in periodontal tissues. High levels of IFN-γ, a strong IDO inducer, were detectable in inflamed gingival tissues.[17,18] IL-1 and TNF-α levels were shown to be elevated in the gingiva of chronic periodontitis and from active periodontitis sites.[19] To the best of our knowledge, the expression and function of IDO in periodontal tissues have not been explored. The aim of this study was to determine IDO expression in healthy and periodontitis gingiva. In addition, we studied IDO expression and the regulation of human gingival fibroblasts (HGFs), one of the most abundant cell types in gingival tissues.

MATERIALS AND METHODS

Gingival Tissue Sample Collection

The study protocol was approved by the ethics committee of the Faculty of Medicine, Chulalongkorn University. Tissue samples were obtained from marginal gingiva excised during tooth extraction or periodontal surgery at the Graduate Periodontology Clinic between April 2006 and December 2007. Written informed consent was obtained prior to tissue collection. For immunohistochemistry, we obtained gingival samples from 12 individuals. Six samples were from healthy gingiva, and six samples were from periodontitis tissues. Healthy gingival samples were collected from sites with clinically healthy gingiva, no bleeding on probing, no radiographic bone loss, and probing depth <4 mm. Periodontitis tissue samples were collected from sites with gingival inflammation, bleeding on probing, radiographic bone loss, and probing depth >5 mm. Tissue samples were washed briefly in normal saline solution, placed in the optimum cutting temperature (OCT) embedding compound, snap-frozen in liquid nitrogen, and stored at –80°C. For fibroblast cell culture, healthy gingival samples were collected from four subjects. Tissues were washed briefly in normal saline solution and placed immediately into tissue culture media. Dulbecco's modified Eagle's medium (DMEM) supplemented with 10% fetal calf serum, gentamicin (50 μg/ml), penicillin G (50 U/ml), streptomycin (50 μg/ml), and fungizone (2.5 μg/ml)[§] was used for tissue collection and cell culture. The samples were kept on ice and processed within a few hours.

Immunohistochemistry

Gingival tissue samples were cut to 5 μm in thickness. Cryosections were fixed with ice-cold acetone for 10 minutes, air-dried, and washed with phosphate buffered saline (pH 7.4). Endogenous peroxidase activity was blocked with 3% hydrogen peroxide for 10 minutes. Immunoperoxidase staining was performed using a commercially available kit.[‖] Non-specific binding was reduced by applying blocking serum for 20 minutes. Sections were incubated overnight at 4°C with purified IDO-specific mouse monoclonal antibody (immunoglobulin G_1; 1 mg/ml diluted at 1:100 in blocking serum) or non-specific mouse antibody.[¶] Antibody binding was detected using an avidin-biotin complex detection technique, following the manufacturer's protocol. Immunostaining was visualized using 3,3-diaminobenzidine chromogen. The slides were counterstained with hematoxylin. For quantitative analysis, the tissue sections were magnified at ×400. Three sample areas within the epithelium were taken from each section. The number of epithelial cells stained positive for IDO was counted, and the percentage of IDO^+ cells was calculated.

Primary Culture of HGFs

The method used to obtain HGF cells from the gingival tissue was described by Murakami et al.[20] Briefly, the biopsy was washed twice with DMEM to remove blood clots and adherent erythrocytes. Then it was cut into fragments of 1 to 3 mm^3 with a sterile scalpel. These tissues were transferred to a 35-mm tissue culture dish containing 2 ml culture medium and incubated at 37°C in a humidified 5% CO_2-air atmosphere. Culture medium was changed twice weekly. When the fibroblast cells surrounding the tissue explants were confluent, they were subcultured into a larger tissue culture dish. HGFs at passages 3 to 6 were used in this study.

Detection of IDO mRNA Expression by Reverse Transcription-Polymerase Chain Reaction (RT-PCR)

HGFs (2.5×10^5 cells/well) were seeded into a six-well tissue culture plate overnight. The cells were stimulated with the following agents: IFN-γ[#] (10 to 1,000 U/ml), TNF-α[**] (0.5 to 50 ng/ml), IL-1β[††] (0.5 to 50 ng/ml), and LPS from *Porphyromonas gingivalis* strain 381[21] (*Pg*LPS; 0.1 to 10 μg/ ml). In addition,

§ Gibco, Grand Island, NY.
‖ VECTASTAIN ABC kit, Vector Laboratories, Burlingame, CA.
¶ Universal negative control mouse antibody, DakoCytomation, Carpinteria, CA.
# R&D Systems, Minneapolis, MN.
** R&D Systems.
†† R&D Systems.

the combination of IFN-γ and each reagent (TNF-α, IL-1β, or *Pg*LPS) was used. Unstimulated HGFs served as a control. After 24 hours, HGFs were harvested to determine IDO expression. Total RNA was extracted, according to the manufacturer's protocol.†† One microgram of total RNA was used for reverse transcription with random hexamer and reverse transcriptase,§§ following the manufacturer's instruction. The cDNA was used for detection of IDO mRNA by PCR. PCR was carried out with PCR mixture containing 15 mM $MgCl_2$, 20 μM IDO primer, 10 mM deoxynucleotide triphosphate, 5 unit/μl Taq polymerase, and the DNA template. The PCR conditions consisted of a first heating step (95°C for 5 minutes), 30 amplification cycles (95°C for 15 seconds, 60°C for 30 seconds, and 70°C for 30 seconds), and one final extension step (72°C for 7 minutes). Specific primer sequences for the gene were as follows: human GAPDH: forward 5′-TCATCTCTGCCCCCTCTGCTG-3′ and reverse 5′-GCCTGCTTCACCACCTTCTTG-3′ (approximate size 400 base pairs [bp]); human IDO: forward 5′-CTTCCTGGTCTCTCTATTGG-3′ and reverse 5′-GAAGTTCCTGTGAGCTGGT-3′ (approximate size 430 bp).[22] PCR products were separated by electrophoresis in a 1.2% agarose gel containing ethidium bromide. GAPDH was used as an internal control. The target bands were visualized with an ultraviolet illuminator and analyzed with image-analysis software.‖‖

Detection of IDO Enzymatic Activity

HGFs (3×10^4 cells/well) were seeded into a 96-well microtiter plate overnight. The cells were stimulated with the following agents: IFN-γ, TNF-α, IL-1β, *Pg*LPS, or their combinations. Unstimulated HGFs served as a control. After 24 and 48 hours, culture supernatants were harvested and assayed for the presence of kynurenine, the first stable catabolite of tryptophan in the kynurenine pathway. Kynurenine was detected by a modified spectrophotometric assay.[23] Briefly, 50 μl 30% trichloroacetic acid was added to 100 μl culture supernatant, vortexed, and centrifuged at 8,000 × g for 5 minutes. Seventy-five microliters of the supernatant was added to an equal volume of Ehrlich reagent (100 mg *p*-dimethylbenzaldehyde and 5 ml glacial acetic acid) in a 96-well microtiter plate. Optical density was measured at 492 nm. A standard curve of defined kynurenine concentration (0 to 100 μM) permitted analysis of unknown samples.

Statistical Analysis

The independent sample *t* test was used to compare the mean percentage of IDO-expressing cells in healthy and periodontitis gingiva. The one-sample *t* test was used to compare the level of IDO activity between samples. Results were expressed as mean ± SE. Data were analyzed using statistical software.¶¶ Statistical differences with a *P* value <0.05 were considered significant.

RESULTS

IDO Expression in Gingival Tissues

The gingival tissue samples were obtained from 12 subjects (six males and six females) with a mean age of 40 ± 12 years (range, 24 to 66 years). We observed IDO expression in healthy gingiva and periodontitis gingiva. Figure 1 shows representative findings. Within epithelium, the number of epithelial cells expressing IDO was lower in healthy tissues (Fig. 1A) than in periodontitis tissues (Fig. 1B). Gingival epithelial cells showed distinct nuclear staining of IDO (Fig. 1C). Within connective tissues, IDO expression was observed in fibroblast cells, endothelial cells, and inflammatory mononuclear cells (Fig. 1D). The number of cells stained positive for IDO was also lower in healthy tissues (Fig. 1E) than in periodontitis tissues (Fig. 1F). The control sections showed no immunoreactivity (Figs. 1G and 1H). Quantitative analysis showed that the percentage of epithelial cells stained positive for IDO was 40.6% ± 8.4% in healthy gingiva compared to 77.7% ± 8.4% in periodontitis gingiva. This difference was statistically significant ($P < 0.001$). The percentage of IDO-expressing cells within connective tissue was not determined; this was due to the close proximity and clustering of cells, which did not allow accurate cell counting.

IDO mRNA Expression by HGFs

RT-PCR analysis was performed to investigate whether inflammatory cytokines and bacterial products induce IDO mRNA expression in HGF cells. Figure 2 depicts a representative RT-PCR result. HGF cells normally did not express detectable levels of IDO mRNA. However, IDO expression was induced upon treatment with IFN-γ, IL-1β, TNF-α, and *Pg*LPS. IFN-γ was the strongest inducer of IDO expression. Relative IDO mRNA expression, as determined by the ratio of IDO mRNA to GAPDH mRNA, is shown in Figure 3. IFN-γ, TNF-α, and *Pg*LPS seemed to induce IDO mRNA expression in a dose-dependent manner. However, stimulation with IL-1β did not show the dose-dependent effect. We also evaluated whether combinations of these cytokines showed an additive effect on IDO induction. HGF cells treated with combinations of IFN-γ and IL-1β, TNF-α, or *Pg*LPS showed increased IDO expression compared to IFN-γ alone (Fig. 4).

†† TRIzol reagent, Invitrogen, Carlsbad, CA.
§§ Improm-II, Promega, Madison, WI.
‖‖ Gene Genius Bio Imaging System, Syngene, Cambridge, U.K.
¶¶ SPSS version 12.0, SPSS, Chicago, IL.

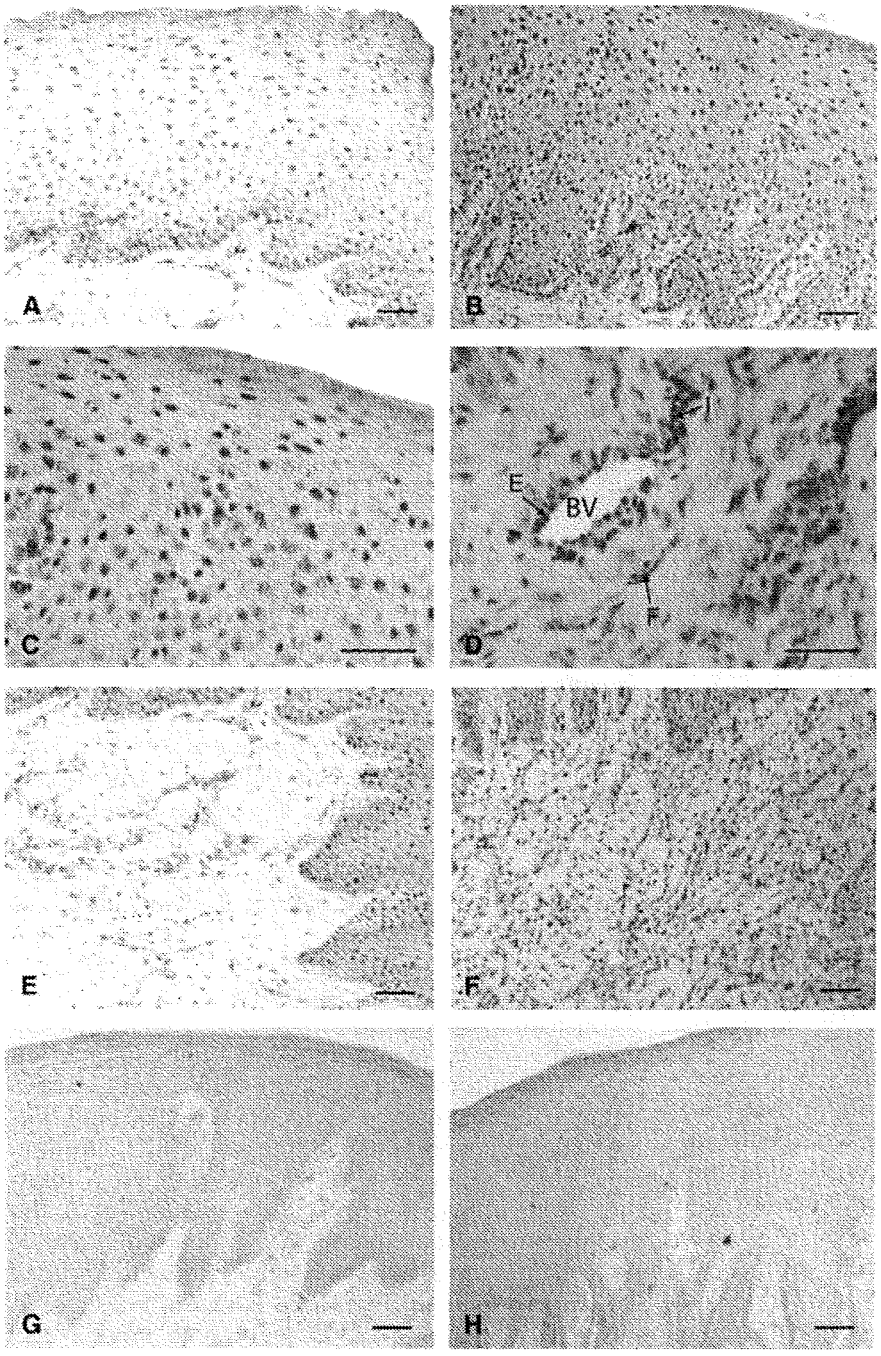

Figure 1.
Immunolocalization of IDO expression in human gingiva. ***A)*** *The epithelium of healthy gingiva.* ***B)*** *The epithelium of periodontitis gingiva. IDO expression was stained with diaminobenzidine and is shown in brown. Cell nuclei were counterstained with hematoxylin and were shown in blue-purple. There were fewer epithelial cells expressing IDO in healthy gingiva than in periodontitis gingiva.* ***C)*** *The nuclear localization of IDO in gingival epithelial cells.* ***D)*** *IDO expression by gingival fibroblasts (F), endothelial cells (E), and inflammatory mononuclear cells (I) (arrows). BV = blood vessel.* ***E)*** *The connective tissue of healthy gingiva.* ***F)*** *The connective tissue of periodontitis gingiva. Cells stained positive for IDO were fewer in healthy tissues than in periodontitis tissues.* ***G)*** *Negative control section of healthy gingiva stained with non-specific immunoglobulin G (IgG).* ***H)*** *Negative control section of periodontitis gingiva stained with non-specific IgG. Scale bars = 50 μm.*

Expression of IDO Activity by HGFs

To evaluate whether HGF cells produced functional IDO, we detected IDO enzymatic activity by measuring the level of kynurenine, which is the first stable catabolite in the metabolic pathway of tryptophan. IDO activity seemed to be increased over time. Significantly increased IDO activity was detected in HGF cells treated with IFN-γ. Increased IDO activity was also observed in HGF cells treated with IL-1β and TNF-α, although it did not reach statistical significance (Fig. 5). The combination of IFN-γ and IL-1β as well as IFN-γ and TNF-α showed significantly higher IDO activity than that of IFN-γ alone (Fig. 6).

DISCUSSION

IDO is an enzyme that metabolizes the amino acid tryptophan. This enzyme has a complex role in immunoregulation in infection, pregnancy, autoimmunity, transplantation, and cancer.[24] In this study we showed that IDO was expressed in human gingiva and may play a role in the pathogenesis of periodontal disease. IDO expression was detected in many cell types within gingival tissues, including epithelial cells, fibroblasts, endothelial cells, and inflammatory mononuclear cells. Within epithelium, the number of epithelial cells expressing IDO was lower in healthy tissues than in periodontitis tissues. Cultured foreskin keratinocytes did not express IDO mRNA unless they were induced by IFN-γ.[25] Tissue samples from inflammatory skin diseases, including psoriasis and atopic dermatitis, showed increased IDO mRNA expression compared to the uninvolved skin.[26] Therefore, the IDO expression in epithelial cells seemed to be upregulated in the presence of inflammation. This was consistent with our findings that IDO expression in epithelium of periodontitis tissues was higher